

國立清華大學生物資訊與結構生物研究所

碩士論文

Institute of Bioinformatics and Structural Biology

National Tsing Hua University

Master Thesis

斑馬魚異種腫瘤移植模型在腫瘤誘發血管新生研究上的應用

The Application of Zebrafish Tumor Xenograft Model in
Tumor-Induced Angiogenesis Research



研 究 生： 童凱澤 (Kai-Che Tung)

學 號： 9780585

指導教授： 莊永仁 博士 (Dr. Yung-Jen Chuang)

中華民國九十九年七月

中文摘要

近年來斑馬魚生物模型被廣泛地應用於癌症研究。其中，斑馬魚異種腫瘤移植模型具有多項獨特優點，包含：斑馬魚飼養維護設備價格便宜、容易操作、可降低實驗藥物的使用量、在基因體學/蛋白質體學研究上有多種工具與方法可以搭配應用，如斑馬魚胚胎原位雜合技術以及免疫螢光染色技術等。不同於其他常見的模式生物，斑馬魚胚胎具有高度透明性，此優點對於在活體上觀測癌症發展以及癌症誘發之血管新生研究有莫大的助益。因此我們利用此模型來研究癌症誘發之血管新生。

卵巢癌近年來為婦科癌症死亡率較高的癌症之一。其惡性程度與腫瘤誘發之血管新生有密切的關係。近年來有報導指出，惡性腫瘤以及其誘發之血管新生與其周遭之 M2 表現型之腫瘤相關巨噬細胞有高度相關性，然而對於腫瘤以及腫瘤相關巨噬細胞之交互作用機制目前仍待釐清。

本篇研究中，我建立了斑馬魚腫瘤異種移植模型，並結合活體外實驗，釐清在腫瘤微環境中惡性腫瘤誘發血管新生的分子機制。在活體外實驗中，我們發現卵巢癌細胞 (SKOV3 cells) 之血管新生因子 (VEGFA) 以及人類組織蛋白酶 S (cathepsin S) 之表現量會在其與 M2 極化之巨噬細胞共同培養後大量上升。而在斑馬魚異種腫瘤移植模型上，我們發現當 M2 極化之巨噬細胞與卵巢癌細胞被共同移植時，腫瘤誘發之血管新生現象會顯著提升。我們的結果顯示腫瘤相關巨噬細胞主要是藉由提升卵巢癌細胞之血管新生相關基因表現，促進腫瘤誘發之血管新生。

Abstract

Zebrafish model have become a powerful tool in cancer research in recent years. The advantages of the zebrafish tumor xenograft model include: low cost, easy experimentation, reduced dosage for drug test, feasibility of various genetics/proteomics approaches such as whole mount in situ hybridization and whole mount immunocytochemistry. Different from other vertebrate organisms, the transparency of zebrafish embryo allowed us to monitor tumor progression and the tumor-induced angiogenesis in live embryos. In addition, zebrafish tumor xenograft model is much more rapid and cheaper than the current mouse model. Thus, here I aimed to use this model in tumor-induced angiogenesis research.

Ovarian carcinoma is considered as one of the leading gynecologic cancers with high mortality rate. The tumor malignancy is highly associated with tumor-induced angiogenesis. The tumor-associated macrophages (TAMs) with M2-like phenotype have been reported with tumor malignancy by promoting tumor-induced angiogenesis; however, the mechanisms of the interaction between cancer cells and macrophages are incompletely understood.

In this study, I established the zebrafish tumor xenograft model to accompany the *in vitro* cell-based assays to elucidate the molecular mechanism of tumor-induced angiogenesis in the cancer microenvironment. I have identified that the VEGFA and cathepsin S are induced in SKOV3 cells after co-cultured with M2-polarized macrophages. Furthermore, the zebrafish tumor xenograft model indicated when co-injected with M2-polarized macrophages, the tumor-induced angiogenesis was significantly increased. In conclusion, my results revealed that the tumor-associated macrophages could trigger the ovarian cancer cells to up-regulate angiogenesis-related genes in promoting tumor-induced angiogenesis.

誌謝

在清華大學的兩年，讓我成長了許多，從似懂非懂的大學生進步到獨立思考的研究生，過程中背後有許多無形的手在支持著我。能夠完成我的碩士論文研究，首先要感謝的是莊永仁老師，帶領我進入科學的思考領域，鼓勵我接觸各種不同的知識，讓我加入系統生物學研究團隊，與資工、電機、化工與統計等各個專長的老師及學長姐合作，學習結合資源與專長，解決有趣的問題，創造一流的研究成果，藉由了解不同領域專家的思考模式，讓自己的專業訓練更加多元，不會侷限在單一領域，這樣的訓練機會是得來不易的，感謝老師讓我有這樣的機會。老師就像一個充滿活力的領航員，帶領實驗室的大家向未知的領域探索，老師永遠走在最前端引領我們思考，加快我們的研究腳步，雖然有時候會跟不上或是迷網，但是可以從中得到獨立思考的機會，整理心情繼續向前，享受收割的喜悅。在結束第一年的合作題目後，老師放手讓我思考屬於我自己的研究計畫，結合所學知識以及技術，嘗試解決複雜的問題，也很高興我能夠達到初步的成果。謝謝莊永仁老師、張文祥老師以及張志隆醫師能夠撥冗指導我，在我有問題的時候提供我思考的方向，並給我正面的鼓勵，讓我有動力繼續向前，在此特別感謝三位老師的指導。

非常感謝在清大求學過程中，幫助過我的所有人。在實驗室中，要特別感謝的是在求學過程指導與協助我的俊傑學長，從一開始的細胞培養、載體構築、酵素活性測試或是之後在斑馬魚血管新生的研究，學長留給我獨立成長的空間，也願意在我有問題的時候花時間坐下來陪我討論，分析可能的問題所在以及實驗設計的邏輯概念。在第一年打下獨立研究的基礎後，第二年已經可以獨立執行要完成的工作以及構想實驗，非常感謝學長讓我有這樣的成長。另外實驗室的大家也在實驗和日常生活中協助我、與我討論與分析，當然也免不了一起在煩悶的實驗室中歡笑與玩樂。無所不知的濠先學長，能解釋各種實驗的原理或是應用，並且帶給我相關的其他背景知識，我從學長那裡學到了很多。感謝孟薇學姐的關心以及打氣，在我喪氣的時候鼓勵我打起精神，以及日常生活對大家無微不至的照顧，讓我們很窩心。感謝捷暉學長的指導，讓我學到相信自己、勇往直前的勇氣，以及苦中作樂的生活態度。怡卉學姐的熱心討論，在實驗上提供了許多的思考方向與選擇，另外也提供了許多吃喝玩樂的好資訊，陪伴我度過在新竹的兩年光陰。相當優秀的威彰學長，

總是能自信的呈現他的研究成果，也獨立的建立各種實用的技術讓大家嘆為觀止。謝謝辛治、仲棋與穆乾三位醫生學長撥空指導我們在臨床相關的經驗，讓我們可以津津有味的聆聽這些珍貴的資訊。中鳳學姐面對生活的態度，一直是我學習的目標。佩慈學姐是實驗室的大幫手，各種大小事都能夠妥善的處理，讓實驗室正常的運作。曉鈞學姐的做事態度，讓我見識到慢工出細活的真諦，做事必須要做到最好才有價值。感謝宏儒在碩士班兩年與我討論與分享經驗，體驗做實驗的酸甜苦辣滋味。感謝芊蕙的陪伴，總是能在大家討論的關鍵時刻做出合理的分析與判斷。另外雖然相處的時間不長，但是在實驗室提供莫大歡樂的宜珊與姿吟，雖然有時候有點吵，但是為莊永仁老師實驗室注入青春的活力，也帶給我許多正面的思考與鼓勵，希望你們在研究生涯能一路順遂。謝謝冠廷在清大的陪伴，陪我一起成長，並為實驗室帶來歡笑。謝謝肇浩與書豪細心照料我們的實驗動物斑馬魚，你們在魚房的工作讓我們有品質穩定的實驗材料可以做實驗，幫了我很大的忙，也謝謝你們在生活上的陪伴。實驗室新進成員婉馨、復誠、譯慶、張捷與正妍，謝謝你們在我口試時的協助，由於相處的時間比較短，我沒能夠幫上你們忙，但是非常歡迎在未來碰到問題時與我或是學長姐討論，希望你們能夠在這個實驗室找到屬於自己的目標。

在碩士班兩年，要感謝生科系排的隊友，讓我可以有一群要好的同伴一起打球，一起出遊，也感謝你們拿下了生科盃冠軍，讓我可以分享這份榮耀。感謝泰毓、偉碩、志泉、冠陵與雅琦這些好朋友，以及擅長思考的室友庚道，在我無助的時候陪伴我，提醒我要出去走走放鬆心情，支持我向自己的理想前進。謝謝張大慈老師實驗室的智彥學長、信杰學長以及偉唐同學，指導我實驗技巧並與我討論實驗。感謝資工系士齊學長以及竹君學姐的指導，在合作計畫的部分，我學到了很多，謝謝你們給我這個機會協助你們。感謝中興陳健尉老師實驗室的學長姐，在我大學生涯為我建立知識以及實驗的良好基礎。感謝國中、高中以及大學朋友們的支持與關心，讓我了解自己不是孤獨的。

最後，感謝我的家人給我的支持與照顧，我給大家添了許多麻煩，感謝你們包容我。謝謝爸爸與媽媽對我生活的貼心叮嚀，辛苦的支持我完成學位。感謝姐姐們與我分享時事與歡樂。謝謝鈺潔對我的體諒，以及你給與我的莫大支持。你們是我背後堅強的堡壘。

感謝這份論文，讓我與幫助我的大家分享我的成果與榮耀。

List of contents

中文摘要	I
Abstract	II
誌謝	III
Abbreviations	VII
1. Introduction	1
1.1 Angiogenesis and current assay models	1
1.2 The advantages of zebrafish model	2
1.3 Ovarian cancer and tumor-associated macrophages	2
1.4 The angiogenesis-related factors in tumor microenvironment	3
1.5 The objective of this study	4
2.1 Zebrafish tumor xenograft model	5
2.2 Cell culture and cell preparation	6
2.3 Construction of nls-mCherry expression vector	6
2.4 CL1-5 cell transfection	7
2.5 Cryosection and histochemistry staining	7
2.6 M1 and M2-polarized macrophage preparation	7
2.7 M2 macrophages and ovarian cancer cell co-culture procedure	7
2.8 Real-time PCR analysis	8
2.9 Western blot	8
2.10 Cathepsin S enzyme kinetic assay	9
2.11 Co-injection of SKOV3 cells and M2-polarized macrophages for tumor-induced neovascularization assay	9
3. Results	10
3.1 The control microspheres stayed immobilized at the injection site and did not induce angiogenesis in zebrafish embryos	10
3.2 Cancer cells could survive and proliferate in zebrafish embryo	10
3.3 Tumor-induced angiogenesis in zebrafish embryos	11
3.4 THP-1 cells were induced to M2-polarized macrophages	12
3.5 The VEGFA and cathepsin S gene expression level of ovarian cancer cells were increased after co-culture with M2 cells	13
3.6 M2-polarized macrophages promote SKOV3 tumor-induced angiogenesis <i>in vivo</i>	14
4. Discussion	15
4.1 Zebrafish tumor xenograft model	15
4.1.1 Micropipettes preparation	15
4.1.2 The host vs. graft rejection of tumor xenograft does not occur in zebrafish xenograft model	16

4.1.3 The choice of xenograft injection site.....	17
4.1.4 The limitations of this model	18
4.2 Tumor-associated macrophages promote ovarian cancer cells induced-angiogenesis	19

List of Tables

Table 1. The sequence of primers used for real-time quantitative PCR.....	25
---	----

List of Figures

Figure 1. Zebrafish tumor xenograft model.....	26
Figure 2. The control microspheres did not migrate or induce angiogenesis in zebrafish.....	27
Figure 3. CL1-5 with endogenous nuclear mCherry indicated human cancer cells could survive and migrate in zebrafish	28
Figure 4. Cancer cell mitosis in zebrafish.....	29
Figure 5. Cancer cell mass was formed at the perivitelline space	30
Figure 6. No cancer-host immune cell interaction was observed around the tumor xenograft	31
Figure 7. The dynamic process of tumor-induced angiogenesis was monitored for up to 80 hours..	32
Figure 8. THP-1 cells were polarized into the M2 macrophages.....	33
Figure 9. Expression level of CTSS was increased in SKOV3 cells co-cultured with polarized M2 macrophages	34
Figure 10. Polarized M2 macrophages effectively promoted SKOV3 cells to induce angiogenesis	35
Figure 11. Proposed model for the role of tumor-associated macrophages in tumor-induced angiogenesis	36

List of Supplemental Figures

Figure S1. The tip of micropipettes was created with blunt end.....	37
Figure S2. Time-course analysis of tumor cell dissemination throughout the perivitelline space.....	38
Figure S3. <i>In vivo</i> cell migration assay	39

Abbreviations

AMC	7-amido-4-methylcoumarin
Amp	Ampicillin
APS	Ammonium persulfate
BSA	Bovine serum albumin
CAM assay	Chick chorioallantoic membrane assay
CTSB	Cathepsin B
CTSS	Cathepsin S
DiI	1,1'-Diiododecyl-3,3,3',3'-tetramethylindocarbocyanine perchlorate
DNA	Deoxyribonucleic acid
DTT	Dithiothreitol
ECL	Enhanced chemiluminescence
ECMs	Extracellular matrices
IL-6	Interleukin-6
IL-12	Interleukin-12
LPS	Lipopolysaccharides
Mrc 1	Mannose receptor 1
PCR	Polymerase chain reaction
PMA	Phorbol myristate acetate
PTU	1-phenyl-2-thio-urea
RIPA buffer	Radioimmunoprecipitation assay buffer
RNA	Ribonucleic acid
SIVs	Sub-intestinal vessels
SDS-PAGE	Sodium dodecyl sulfate polyacrylamide gel electrophoresis
Sr 1	Scavenger receptor 1
TAMs	Tumor-associated macrophages
TBST	Tris-Buffered Saline Tween-20
TEMED	Tetramethylethylenediamine
TNF- α	Tumor necrosis factor-alpha
VEGFA	Vascular endothelial growth factor A
Z-VVR-AMC	Benzyloxycarbonyl-valine-valine-arginine-7-amido-4-methylcoumarin

1. Introduction

1.1 Angiogenesis and current assay models

Angiogenesis, the development and formation of new blood vessels from pre-existing blood vessels, is an important topic in cancer research^{1,2}. The new blood vessels formation is known to support the growing tumor mass with continuous oxygen, nutrition and growth factors supply, which is critical for cancer cell survival, proliferation and migration. Anti-angiogenesis is thus targeted for anti-cancer drug development.

Throughout the years, many angiogenesis assays have been developed for preclinical cancer research. Some *in vitro* assays are designed with experiment conditions to mimic the *in vivo* environment. Although various angiogenesis factors are successfully identified by *in vitro* angiogenesis assays, these *in vitro* assays can only focus on a narrow aspect of endothelial cells physiology, such as the migration, proliferation and differentiation^{4,5}. On the other hand, it shall be noted that these assays are unable to recreate the true angiogenic microenvironment *in vivo*. For example, cancer cells usually do not directly interact with endothelial cell in these assays, or the components of the assay only represent part of the *in vivo* conditions.

In vivo angiogenesis assay has thus been developed and used in cancer research because it provides a system more close to the physiological conditions in living beings⁵. However, there are some limitations of these complex and expansive assays. For example, the popular chick chorioallantoic membrane (CAM) assay is often used to analyze the density, branch point and the length of the vessels, but it cannot be used to trace the dynamic endothelial cell behavior or capillaries growth with high-resolution. Another common *in vivo* model, the nude mouse model, is a powerful tool because the physiological system of mice is similar to human; however, this model is a high-cost assay system. The mouse study usually requires a lengthy observation time and needs to sacrifice a large number of mice to analyze the effect by tissue section. Therefore, a new *in vivo* model that could be used to conveniently study angiogenesis in detail and to reduce the assay cost

and time is still much needed.

1.2 The advantages of zebrafish model

Zebrafish model have become a popular tool in human disease models in recent years. There are many transgenic strains available, and can be easily maintained in the laboratory. Other advantages of the zebrafish xenograft model include: the husbandry infrastructure are inexpensive, reduced cost on the drug used per experiment, direct visualization of cancer cell behavior, feasibility of various genetics/proteomics approaches like whole mount in situ hybridization or whole mount immunocytochemistry ⁶. Furthermore, zebrafish intersegmental vessels (ISV) development assay and sub-intestinal veins (SIV) assay have been successfully used to study the function of angiogenesis factor *in vivo* ⁷. Recently, the zebrafish tumor xenograft model has emerged as an alternative and increasingly popular system in cancer research ^{6,8-11}. Different from other vertebrate organisms, the transparency of zebrafish embryos allow us to monitor tumor progression and angiogenesis in live embryos under confocal microscope ^{6,8-10}. Current bio-imaging technology could also allow real-time observation on new vessel development in the around the tumor in live zebrafish.

1.3 Ovarian cancer and tumor-associated macrophages

Ovarian carcinoma is considered as one of the leading gynecologic cancers with high mortality rate ². The estimated 5-year relapse-free survival rate of ovarian carcinoma is only 30% ¹². Early-stage ovarian carcinoma is generally asymptomatic, and 70% of the patients are diagnosed at stage III/IV ¹³. The stage III/IV ovarian cancers are often presented with massive ascites, and the accumulation of fluid is considered closely associated with tumor-induced angiogenesis and increased vascular permeability in peritoneal micro-vasculatures ^{13,14}. Thus, blocking tumor-induced angiogenesis is an important objective in ovarian cancer therapy.

Recently, the microenvironment of tumor growth has been studied extensively ^{15,16}, with a

focus on the complex interaction between cancer cells and resident stromal cells. A critical type of stromal cells around the solid tumor is tumor-associated macrophages (TAMs)¹⁷⁻²⁰. Over the past decade, TAMs are found to promote tumor growth and progression by facilitating angiogenesis and tumor cells invasion. Clinical data indicate that the tumor microenvironment with abundant TAMs is linked to poor prognosis of various cancers, including breast, ovarian and pancreatic cancers²¹⁻²³. Macrophages are innate immune cell with high degree of heterogeneity, and its functional roles can be changed and are associated with their location environment^{19,21,22,24}. Recent studies have reported that macrophages under lipopolysaccharides (LPS) stimulation can be polarized to M1 macrophages, which carry inflammatory and anti-tumor activities; when they are exposed to Th2-cytokine (IL-4 and IL-13), they will polarized into M2 macrophages, which moderate the inflammatory response, eliminate cell wastes, and promote angiogenesis and tissue remodelling^{16,25}. The M2-phenotype macrophages can express high levels of M2-specific genes, such as mannose receptor 1 (Mrc1) and low expression of TNF- α and IL-12^{26,27}. Interestingly, the TAMs with M2-like phenotype were found to support tumor growth^{26,27}. In addition, previous studies have revealed the M2-phenotype TAMs are involved in extracellular matrix (ECM) remodelling, which promote endothelial cells migration to form new vessels^{15-17,20}. The comprehensive understanding of the molecular mechanism of tumor-induced angiogenesis by the interaction between TAMs and cancer cells in cancer development microenvironment will advance the ongoing cancer research to develop novel therapy.

1.4 The angiogenesis-related factors in tumor microenvironment

The most important factor involved in tumor-induced angiogenesis is vascular endothelial growth factor (VEGF)²⁸. Clinical data indicated a high VEGF expression level detected in ovarian carcinoma and in patient's ascites^{29,30}. A body of evidences show that the VEGF-induced signal transduction stimulates endothelial cell proliferation, migration, and survival³¹. Furthermore, it has been reported that VEGF induce vessels sprouting by up-regulating other cell migration factors,

such as integrin receptors in tumor-induced angiogenesis³. Besides VEGF, there are other pro-angiogenic factors involved in tumor-induced angiogenesis. One interesting group of these factors are the 11 human cysteine cathepsin proteases (Cts) (B, C, H, F, K, L, O, S, V, W, and X/Z), which are known to involve in protein degradation in the lysosomes, protein processing or antigen presentation^{32,33}. Some clinical studies have shown that up-regulation of cathepsin B and S are detected in various types of cancers^{34,35}. Interestingly, recent studies also showed that these cysteine cathepsins are involved in the degradation of extracellular matrix macromolecules and in the activation of pro-enzymes in tumor microenvironment by secreted into the extracellular matrix or onto the cell surface³⁶⁻³⁸.

1.5 The objective of this study

Most of the published studies have only investigated the correlation between ovarian cancer outcomes and TAMs, or the tumor malignance with cathepsin activity separately. To our knowledge, there is no study to investigate the connection between TAMs and cathepsins in tumor-induced angiogenesis of ovarian cancers. Here, we established the zebrafish tumor xenograft model to accompany the *in vitro* cell-based assays to elucidate the molecular mechanism of tumor-induced angiogenesis. We found under the co-culture condition with polarized M2 macrophage, the gene expression level of VEGFA and cathepsins in SKOV3 ovarian cells increased significantly, and the protein level of active cathepsin S was also markedly increased. Moreover, we co-transplanted SKOV3 cells and M2-polarized macrophages into zebrafish embryos, and found the tumor-induced angiogenesis were enhanced significantly as compared to either SKOV3 cells or M2 macrophage alone. Taken together, this study demonstrated that M2-polarized macrophages could promote tumor-induced angiogenesis by up-regulating factors like cathepsins in the ovarian cancer cell mass. Our findings imply that the depletion or blockade of TAM-dependent cathepsin production in tumor microenvironment might reduce tumor-induced angiogenesis, which can become a worthy strategy in developing novel ovarian cancer therapy.

2. Materials and Methods

2.1 Zebrafish tumor xenograft model.

Zebrafish (*Danio rerio*) Tg(*kdr:EGFP*) and Tg(*lyz:EGFP*) (a kind gift from Dr. Phil Crosier; The University of Auckland, New Zealand) strains were maintained under standard laboratory conditions. Fertilized zebrafish eggs were incubated at 28.5°C in sea salt buffered water. At 24 hours post-fertilization, the zebrafish eggs were incubated in 0.006% sea salt water containing 0.2 mM 1-phenyl-2-thio-urea (PTU, Sigma) to prevent pigmentation and incubated for further 24 hours at incubator. The 2 days post-fertilization zebrafish eggs were dechorionated by suspending in 2 mg/ml pronase (Sigma) for 3 minutes, then changed to fresh sea salt water containing PTU and flushed with the dropper to remove the chorion. The dechorionated embryos were anesthetized with 0.02 mg/ml tricaine (MS-222, Sigma), and arranged with the correctly orientated on the agarose-modified microinjection plates. The cells-injected needles were prepared from borosilicate glass needles (with inner diameter 0.53 mm, outer diameter 1.14 mm; Drummond). The parameters of the pipette puller were: Pressure: 500, Heat: +10, Pull: 0, Velocity: 50, Delay time: 200. The inner diameter of the needle opening was about 20 µm. Cancer cells were aspirated by using a nanoliter injector (Drummond) equipped with a borosilicate glass needle. Aspiration should be slow so that cells will not block the pipette. DiI-labeled cells were injected into the perivitelline space of 2 days post-fertilization zebrafish embryos (Fig. 1). It shall be noted that the embryos will be killed when the cancer cells were injected in yolk or other sites. At 2 hours post-injection, the transplanted embryos were checked for correct injection using fluorescent microscope. The embryos with successful transplant were then incubated in 0.006% sea salt water containing 0.2 mM PTU at 28.5°C. The transplanted embryos were anesthetized by 0.02 mg/ml tricaine and embedded in lateral orientation in 1% low-melting agarose, and examined by Nikon A1R confocal microscope for the following days.

2.2 Cell culture and cell preparation

Human non-small cell lung cancer cell line CL1-0 and CL1-5 and human melanoma cell line A2058 were generous gifts from Dr. Wun-Shaing Chang (National Health Research Institutes, Taiwan). Human ovarian adenocarcinoma cell line SKOV3 was generous gifts from Dr. Chih-Long Chang (Mackay Memorial Hospital, Taiwan). CL1-0, CL1-5 cells and SKOV3 cells were cultured in RPMI 1640 medium (Invitrogen) supplemented with 10% FBS, 100 mg/ml penicillin, and 100 mg/ml streptomycin. A2058 cells were cultured in Dulbecco's modified Eagle's medium (Invitrogen) supplemented with 10% FBS, 100 mg/ml penicillin, and 100 mg/ml streptomycin. THP-1 human monocytic cell line (American Type Culture Collection) were cultured in RPMI 1640 medium (Invitrogen) supplemented with 2.5 g/l glucose, 10 mM HEPES, 1 mM sodium pyruvate, 10% FBS, 100 mg/ml penicillin, 100 mg/ml streptomycin and 0.05 mM 2-mercaptoethanol. Before microinjection, the cancer cells were labeled with 3.75 μ g/ml of 1,1'-Diiododecyl-3,3,3',3'-tetramethylindocarbocyanine perchlorate (DiI, Invitrogen) for 30 minutes. The labeled cells were thoroughly washed 3 times with PBS, counted by hemocytometer, and suspended 8×10^4 cells/ μ l in matrigel (Trevigen).

2.3 Construction of nls-mCherry expression vector

The nuclear-localized mCherry sequence was sub-cloned from pME-nlsmCherry by PCR amplification using primers: 5'-GGATCCATGGCTCCAAAGAAGAAGCGTA-3' (forward) with BamHI restrict enzyme cutting site and 5'-GAATTCTTACTTGTACAGCTCGTCCATG-3' (Reverse) with EcoRI restrict enzyme cutting site. PCR was performed by using Phusion™ DNA polymerase (Finnzymes) and checked by using DNA agarose gel electrophoresis. The PCR product with correct size was digested from the gel and eluted by using gel elution kit (Quiagen). The PCR products were constructed into pGEMTeasy vector (Promega) and sub-cloned into pCMV-Tag4a (Stratagene), which contain the kanamycin resistance gene. The pCMV-nlsmCherry plasmid was sequence verified.

2.4 CL1-5 cell transfection

CL1-5 cells were seeded 5×10^4 cells/ μ l in 24-well plate overnight at 37°C in incubator. Before performing cell transfection, the medium was replaced with serum/antibiotics free medium. An amount of 0.8 μ g pCMV-nlsmCherry and 0.5 μ l Lipofectamine™ 2000 reagent were diluted in 50 μ l Opti-MEM® reduced serum medium (Invitrogen) separately. The reagents were incubated for 5 minutes at room temperature and mix for another 20 minutes at room temperature. The mixture were added into medium and incubated at 37°C in incubator. At 4 hours post-transfection, the medium was changed with complete medium. For stable clone selection, complete medium containing 800 μ g/ml G418 were used to select cells that express kanamycin resistance gene.

2.5 Cryosection and histochemistry staining

Transplanted embryos were killed by placed into 4% paraformaldehyde at 4°C overnight. The embryos were washed with PBST for 3 times and infiltrated in OCT. The 16 μ m thick cryosections were processed and placed on charged slides (Thermo). The fluorescence of samples was examined by confocal microscope. The slides were then stained with Hematoxylin and Eosin.

2.6 M1 and M2-polarized macrophage preparation

The different polarized macrophages were prepared from THP-1 cells by following Tjiu's procedure³⁹. For M1-polarized macrophages, 1×10^7 THP-1 cells were treated with 200 ng/ml phorbol myristate acetate (PMA) for 6 hours and cultured with PMA plus 100 ng/ml LPS for the following 18 hours. For M2-polarized macrophages, 1×10^7 THP-1 cells were treated with 200 ng/ml PMA 6 hours and then cultured with PMA plus 20 ng/ml IL-4 and 20 ng/ml IL-13 for another 18 hours.

2.7 M2 macrophages and ovarian cancer cell co-culture procedure

SKOV3 cells were seeded 2.5×10^5 cells/well in 6-well plate overnight. THP-1 cells were

seeded 1×10^6 cells/well and treated with 200 ng/ml PMA and seeded into the 6 well Hanging Cell Culture Insert (0.4 μ m pore size, Millipore) for 6 hours, and then cultured with PMA plus 20 ng/ml IL-4 and 20 ng/ml IL-13 for another 18 hours at 37°C in incubator. M2-polarized cells were thoroughly washed 3 times to remove all PMA and cytokines contained medium. Then the macrophages were co-cultured with SKOV3 cells in RPMI serum free medium without direct contact. The insert wells were removed and the SKOV3 cells were harvested the RNA or protein for real-time quantitative PCR, Western blot or enzyme kinetic analysis.

2.8 Real-time PCR analysis

After co-culture, total RNAs of SKOV3 cells were harvested using TRIZOL reagent (Invitrogen) according to the manufacturer's protocol. An amount of 1.5 μ g total RNAs were treated with deoxyribonuclease I (Invitrogen) to eliminate genomic DNA contamination in following experiment. The products were then reverse-transcribed using Superscript III (Invitrogen) and Oligo(dt)₁₂₋₁₈. The real-time quantitative PCR were performed with SYBR green master mix (Applied Biosystems) and Applied Biosystems 7500 Real-Time PCR System. The primers used in this study are listed in Table 1.

2.9 Western blot

After co-culture, RIPA buffer containing 1 mM PMSF, 2 mM DTT and cocktail were used to lyse the cancer cells. Whole cell extracts were prepared and quantitated by Bradford assay. SDS-PAGE was performed with Trans-Blot[®] Electrophoretic Transfer Cell Instruction Manual (Bio-Rad). The gel was transfered (70 min at 400mA) onto 0.45 μ m PVDF membrane (Millipore) in transfer buffer (25 mM Tris-Base, 192 mM glycine, 20 % methanol without SDS) using Tank Transfer Systems (Bio-Rad). The membranes were blocked in 5% skim milk or 3% bovine serum albumin in TBST (200mM Tris-base, 1.5M NaCl, pH 7.6, 0.002% Tween-20) 1 hour in room temperature. Immunoblotting used primary antibody, cathepsin S (Santa Cruz) and β -actin (Santa

Cruz) at 4°C overnight. The primary antibody was removed and the membrane was washed 3 times with 10 ml TBST for 10 minutes. The HRP-conjugated secondary antibody was used in 5% skim milk or 3% bovine serum albumin in TBST at room temperature for 1 hour. The blots were developed using ECL chemiluminescence systems and the images were exposed to films.

2.10 Cathepsin S enzyme kinetic assay

The assay procedure was derived from Dr. Margaret DT Chang's lab (National Tsing Hua University, Taiwan). The benzyloxycarbonyl-valine-valine-arginine-7-amido-4-methylcoumarin (Z-VVR-AMC) was purchased from Bachem (Torrance, CA) and used as the cathepsin S substrate. In cathepsin S kinetic assay, 15 µg total cell lysate were added to kinetic assay buffer (50 mM MES, pH 6.5, 1 mM DTT and 2.5 mM EDTA) and incubated for 10 minutes at 37°C. The substrate Z-VVR-AMC was then added to a final concentration of 5 µM. After adding the substrate, 7-amido-4-methylcoumarin (AMC) was released by hydrolysis of the Z-VVR-AMC and the fluorescence was detected with VICTOR3 Multilabel Plate Reader (PerkinElmer) using excitation wavelengths of 370 nm and emission wavelengths of 455 nm.

2.11 Co-injection of SKOV3 cells and M2-polarized macrophages for tumor-induced neovascularization assay

SKOV3 cells were labeled with DiI before the cells were harvested. M2-polarized macrophages were washed 3 times and incubated in 5 ml PBS for 30 min to reduce the adhesion ability. The cell scraper was used to harvest the cells. The harvested cells were counted by hemocytometer, and suspended 8×10^4 cells/µl in matrigel. The SKOV3 cells and M2-polarized macrophages were prepared as 1:1 proportion mix. The cells were injected into the perivitelline space of 2 days post-fertilization zebrafish embryos, and examined by Nikon A1R confocal microscope at 3 days post-injection.

3. Results

3.1 The control microspheres stayed immobilized at the injection site and did not induce angiogenesis in zebrafish embryos

As a control experiment, fluorescent microspheres were injected into the perivitelline space of the zebrafish embryo. The 10 μm orange (540/560) fluorescent microspheres are chosen to mimic the cancer cell size and density. When the fluorescent microspheres were transplanted into zebrafish, they stayed at the injection site and the zebrafish sub-intestinal vessels (SIVs) developed normally. No abnormal neovascularization was observed up to 4 dpi. (Fig. 2)

3.2 Cancer cells could survive and proliferate in zebrafish embryo

In this assay, I tested whether human cancer cells could survive in zebrafish. The stable clone of mCherry-labeled cancer cell was first generated. The nuclear-localized mCherry DNA sequence from the pME-nlsmCherry plasmid was sub-cloned into the pCMV-Tag-4a plasmid (Fig. 3A). The resulting pCMV-nlsmCherry was then transfected into CL1-5 cells, a human non-small lung cancer cell line. The cells expressing stable nuclear mCherry gene were selected by G418 treatment for 2 months (Fig. 3B). The resulting stable clone of mCherry-labeled cell line was then injected into zebrafish embryos. Up to 5 days post-injection, the mCherry-labeled cells could still be detected at the anterior and posterior regions in the live zebrafish embryos (Fig. 3C). These data demonstrate that human cancer cells could indeed survive in zebrafish embryo. Knowing that, we then switched to the easier DiI labeled method for the subsequent experiments so any kind of human cancer cell lines could be labeled and tracked in zebrafish. As demonstrated in previous study by Nicoli et al, DiI is a dialkylaminostyryl dye that does not affect cell viability or basic physiological properties⁴⁰, and the labeled cells could remain viable for up to 4 weeks in culture and up to one year *in vivo*⁴¹.

In my cell tracking experiments, I monitored cancer cell mitosis by the Nikon A1R real-time confocal system. At 2 days post-injection, the cell mitosis process was tracked in blood islands via

time lapsed images (Fig. 4). I captured the image of a DiI-labeled CL1-5 cell when it was dividing into two daughter cells across a 6-hour period. In an additional test, I injected approximately 20 DiI-labeled human melanoma cells (A2058) mixed with matrigel into the perivitelline space of another zebrafish embryo to generate a small cancer cell mass. The injected cells were tracked by real-time confocal microscopy up to 5 days. As shown in Fig. 5A, the cancer cell mass gradually formed and increased in size at the injection site (Fig. 5). These results indicate that the human cancer cells could proliferate in zebrafish embryo.

In most cancer animal models, the xenograft rejection by the host is always a major concern during experiment. If the host's immune system attacks the foreign cells, it could result in either failed experiments or misleading conclusion. To investigate whether this phenomenon also appear in our zebrafish model, I transplanted CL1-5 cells into the Tg(*lyz:EGFP*) zebrafish embryos, which carry endogenous fluorescent macrophages. The Tg(*lyz:EGFP*) strain was originally created by Phil Crosier's group in 2006⁴². The enhanced green fluorescent protein is driven by *lysC* promoter, which has been demonstrated to express specifically in a subset of zebrafish macrophages and likely also granulocytes⁴³. Thus, I used the Tg(*lyz:EGFP*) zebrafish to examine the interaction between the human cancer xenograft cells and the zebrafish host immune cells. For this assay, the DiI-labeled CL1-5 cells were injected into perivitelline space of 2 days post-fertilization embryos. The transplanted embryos were examined by the Nikon A1R confocal microscopy. Interestingly, I found no signs of interaction between the CL1-5 xenograft cells and the host myelomonocytic cells. The EGFP-labeled macrophages migrated normally in zebrafish, with no sign of recruitment to the tumor cell mass (Fig. 6). This result indicates that, at this developmental stage, the host immune system might not attack the xenograft cells in our zebrafish tumor xenograft model.

3.3 Tumor-induced angiogenesis in zebrafish embryos

The transparency of the zebrafish embryo, in combination with the transgenic vascular

fluorescent zebrafish line, makes it a powerful model for analyzing tumor-induced angiogenesis study. Since I have demonstrated human cancer cells could survive and proliferate in zebrafish embryo, I next use this zebrafish xenograft model to examine the tumor-induced angiogenesis. The DiI-labeled CL1-5 cells were again injected into the perivitelline space near the sub-intestinal vessels. The tumor-induced angiogenesis were tracked for 30 hours by real-time confocal microscope. As shown in the time lapse imaging data, the growth of the new vessels was clearly observed (Fig. 7). I also found the injected cell mass successfully induced the highly disorganized expansion of the SIV vessels around the cancer cell mass. Strikingly, the dynamic fusion process of 2 tip cells on different growing vessels was captured. At 4 days post-injection, the pattern of the sub-intestinal vessels was evidently perturbed by the tumor cell mass.

3.4 THP-1 cells were induced to M2-polarized macrophages

After I established the zebrafish tumor xenograft model, I used the system to further study the interaction between tumor-associated macrophages and cancer cells in the microenvironment. Macrophages are highly heterogeneous cells with various functional phenotypes associated with their microenvironment settings and stimulation ⁴⁴. Recent studies had reported that tumor-associated macrophages have an M2-like phenotype ²⁶. In Tjiu's study, they polarized the THP-1 cells into M1 and M2 subtype macrophages by treated the THP-1 cells with phorbol myristate acetate (PMA) and then with either the Th1 (LPS and IFN- γ) or Th2 (IL-4/IL-13) cytokines. Following their protocol, I polarized the THP-1 cells into M2-phenotype macrophages for the subsequent assays (Fig. 8A). The THP-1 cells were treated with 200 ng/ml PMA for 6 hours, followed by treatment with IL-4 (20 ng/ml) and IL-13 (20 ng/ml) for 18 hours. The resulting cells would attach to the dish and differentiated to M2-polarized cells. As a validation, the gene expression level of M1 and M2-polarized macrophage marker genes were analyzed (Fig. 8B, C). The M2-polarized macrophage showed a high expression level of M2 marker genes. The mannose receptor (Mrc 1) was increased by 21.7-fold and the scavenger receptor (Sr 1) was increased by

3.3-fold, respectively; and the M1 marker genes, TNF- α , IL-6 and IL-12, in M2 macrophages were expressed at levels around 30-46 folds lower than M1-polarized macrophages. The results are consistent with the previous study³⁹. Hereafter, I used these THP-1 polarized M2 macrophages for the subsequent experiments.

3.5 The VEGFA and cathepsin S gene expression level of ovarian cancer cells were increased after co-culture with M2 cells

In order to investigate the interaction between ovarian cancer cells and tumor-associated macrophage, I co-cultured SKOV3, a human ovarian adenocarcinoma cell line, and M2-polarized macrophages in a co-culture system with no direct cell-cell contact. After incubation, M2 cells were discarded and the total RNAs of SKOV3 cells were isolated to determine the VEGFA and cathepsins gene expression level (Fig. 9A). In our co-culture system, the gene expression level of VEGFA was increased by 7-fold, which is consistent with previous studies^{18,39,45}. I then examined the gene expression level of selected cathepsins after co-culture. In addition, the real-time quantitative PCR data indicate that, after co-cultured with M2-polarized macrophages, SKOV3 cells would up-regulate the gene expression levels of cathepsin B and S by 1.6-fold and 12.5-fold, respectively (Fig. 9B). Interestingly, this data also showed the expression level of cathepsin S was significantly higher than cathepsin B. To verify this at the protein level, I further examined the protein expression level of cathepsin S by Western blot. I found the active form of cathepsin S was indeed increased in SKOV3 cells after co-cultured with the M2-polarized macrophages (Fig. 9C). Furthermore, cathepsin S kinetic assay indicate that the cathepsin S activation was also increased in the SKOV3 cells (Fig. 9D). Taken together, these *in vitro* data suggest that the M2-polarized macrophages could trigger the SKOV3 cells to up-regulate angiogenesis-related genes expression, which indicate tumor-associated macrophages may also play a critical role in promoting tumor angiogenesis in ovarian cancer.

3.6 M2-polarized macrophages promote SKOV3 tumor-induced angiogenesis

in vivo

In this assay, I tested whether M2-polarized macrophages promote SKOV3 tumor-induced angiogenesis *in vivo*. The DiI-labeled SKOV3 cells and M2-polarized macrophages were co-injected into the perivitelline space of the zebrafish embryos. At 3 days post-injection, the tumor-induced angiogenesis was examined (Fig. 10A). The quantitative data indicated that co-injection of M2-polarized macrophages and SKOV3 could enhanced vessels length and number of branch points within the cancer cell mass, as compared to either the SKOV3 or M2-polarized macrophages only (Fig. 10B, 10C). The total vessels length and branch points in co-injection group increased by 1.3-fold and 1.6-fold, respectively, compared with that of control SKOV3 group. Thus, our *in vitro* and *in vivo* data both support that polarized M2 macrophages could promote tumor angiogenesis of ovarian cancer.



4. Discussion

In this study, I first established the zebrafish tumor xenograft model for human cancer research. I then applied this model system to study the connection between tumor-associated macrophages and cathepsin in term of tumor-induced angiogenesis of ovarian cancer. I found the gene expression levels of VEGFA and cathepsin S in SKOV3 cells are increased after co-cultured with M2-polarized macrophages *in vitro*, and the *in vivo* analysis further validated that M2-polarized macrophages indeed play a role in tumor-induced angiogenesis in the zebrafish tumor xenograft model. I thus revealed that cathepsin S has an important functional role during SKOV3-induced angiogenesis via paracrine interaction with M2-polarized macrophages (Fig. 11).

4.1 Zebrafish tumor xenograft model

As shown in this study, zebrafish xenograft model is a simple, fast and highly efficiency animal model for angiogenesis assay in cancer research. Based on my results, the tumor-induced angiogenesis experiment could be completed within 3 to 4 days post-injection. That is much faster and easier than other vertebrate animal models like chick chorioallantoic membrane (CAM) model or mouse xenograft model. Using the zebrafish tumor xenograft model, we could compare the ability to induce tumor-induced angiogenesis of different human cancer cells. The critical issues involved in the model set up are discussed as below.

4.1.1 Micropipettes preparation

In zebrafish tumor xenograft model, the proper preparation of micropipettes was critical to the success of effective cancer cells transplantation. The parameters of the micropipettes shall depend on the specific application. Along with different parameter setting, there are different kinds of tip size, taper length and resistance. For successful recovery of the zebrafish peridermal membrane,

minimal trauma to the embryo was important. This implies the outer diameter of the micropipette shall be as small as possible. On the other hand, the inner diameter of the tip should be large enough to allow smooth aspiration of the cancer cells suspended in viscous matrigel solution. Taken together, preliminary testing is required to ensure the custom-made pipette could penetrate the peridermal membrane of the embryo, and be large enough to aspirate the selected cancer cells. The size, shape and other parameters of the final micropipette can only be created from trial and error by testing different combination of filament and parameters.

With the suitable micropipette in hand, people also need to pay attention to the zebrafish host subject because the zebrafish embryonic yolk membrane is very frail. To minimize the damage, I found the tip of micropipettes should not be beveled. In my zebrafish tumor xenograft model, I found pipettes with blunt end were most suitable, which is different from what were reported in the published protocols. In my preparation, the blunt end of pipette was created by "glass-on-glass" method. This is done by putting another pipette above the location of the cutting site, and moves with a fluid motion to push the top of the taper back and away (Fig. S1). With optimised parameter setting to pull the needle and the blunt end shaping of micropipette tip, high success rate of the tumor xenograft transplantation could be anticipated.

4.1.2 The host vs. graft rejection of tumor xenograft does not occur in zebrafish xenograft model

The xenograft rejection by the host immune system could be a big problem in xenograft transplantation since the foreign cells might activate the host's adaptive immune system^{46,47}. In mouse xenograft model, researchers always need to use severe combined immunodeficiency (SCID) mice or have the recipient mice be treated with radiation to destroy the bone marrow before the experiment. Interestingly, the xenograft rejection did not occur in our system. It has been shown that, the zebrafish adaptive immune system will not become mature until 4 to 6 weeks post-fertilization⁴⁸, and pervious studies figured out that the transplantation of adult donor's kidney marrow stem cells

to embryos was not induced the graft rejection in zebrafish ⁴⁹. That is an important advantage of using zebrafish embryos as the host for this tumor xenograft model.

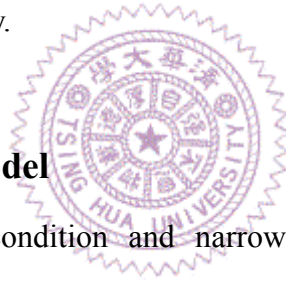
On the other hand, recent studies have shown that macrophages play a critical role in initial xenograft rejection ⁵⁰. To examine whether macrophages are recruited to the tumor xenograft, I injected the human cancer cells into the 2-days-old Tg(*lyz:EGFP*) zebrafish embryos to examine the interaction between macrophages and the xenograft cells. I found the macrophages would not attack the xenograft cells within 2 days post-injection. This result indicates the macrophages of the developing zebrafish embryos shall not initiate xenograft rejection in zebrafish xenograft model.

4.1.3 The choice of xenograft injection site

The injection site of the xenograft cells mass is an interesting issue in setting up the model. In my preliminary trails, I tried to inject the cells at different sites, including the perivitelline space and inside the yolk. I found the perivitelline space is most optimal for my study. In Nicoli's study, they described the perivitelline space to be the space between the periderm and the yolk syncytial layer ¹⁰. However, there are two possible injection sites in this region, one is at posterior yolk sac near the sub-intestinal vessels, and the other is near the duct of Cuvier (it is also known as the common cardinal vein). In my study, I mainly chose the site near the sub-intestinal vessels to monitor the tumor-induced angiogenesis, but I also found the site near the duct of Cuvier is more suitable for the *in vivo* migration assay.

At 48 hours post-fertilization, the circulatory system of a zebrafish embryo at the end point of the duct of Cuvier is an open vessel ⁵¹. When cancer cells are suspended in PBS and injected into the site near the duct of Cuvier, the cells have better chance to show a higher mobility to reach other anatomic sites of the fish host. With this characteristic, I tried to establish the *in vivo* cell migration assay in my model system. Human non-small cell lung cancer cell lines CL1-0 and CL1-5 are the cells of choice for this assay. CL1-0 and CL1-5 are derived from the same lung cancer cell line but with different mobility and invasion ability. Therefore, I used these two cell lines to test our

zebrafish xenograft model to see whether this system can be used to distinguish the different cell mobility and invasion ability *in vivo*. In my experiments, tumor cells disseminated from the perivitelline space was traced by real-time confocal microscopy (Fig S2). Quantification of migrated cells by image analysis in tail region clearly showed that this assay can distinguish different cell mobility just like the *in vitro* assay (Fig S3). This means we may use this model to analyze the molecular mechanism of cell migration of any other human cancer cells. For instance, there are many genes known to regulate cell migration ability. Cancer cell lines can be modified by mutation or gene knockdown to study the gene function on the migration ability as compared with the parental cells in this zebrafish model. I believe my zebrafish tumor xenograft model is more rapid and cheaper than the current mouse model. Most importantly, cell behavior can be examined real-time in high magnification *in vivo*, and structure of membrane protrusion of the cells can also be traced as demonstrated in this study.



4.1.4 The limitations of this model

The abnormal cells growth condition and narrow observation window are the major limitations of this model. In my zebrafish tumor xenograft model, the implanted embryos were kept at 28.5°C, and this condition is lower than the physiological body temperature in mammals. Although the cancer cells in my model did not grow at the native physiological condition, the cell could still survive and proliferate in the zebrafish embryos within 5 days post-injection (Fig 3,4,5). Unfortunately, in the mCherry-labeled CL1-5 transplantation experiment, although the mCherry signals can be detected by microscope until 8 days post-injection, the mCherry signals would diminish gradually compared to the early time points. This phenomenon may be caused by the change of cell physiology at late stage embryos. Because the growth condition in zebrafish is not suitable for cancer cells, it may interfere with the cells survival at long term. Thus, the main drawback of this model is that it cannot exceed 6 days post-fertilization. This could translate to the single migrating cancer cell cannot form a metastatic cell mass distant from the primary tumor mass.

The narrow observation window was another major limitation of this model. Because the yolk is turbid and its opacity would affect light transmission, such factors would affect the depth of penetration of the lasers to excite the reporter fluorescent protein within the cancer cells in the embryo. If the target cells within the embryos travel too deep into the tissue (beyond 200 μm), the image quality would decrease significantly or the cancer cells cannot be observed under current confocal microscope system.

4.2 Tumor-associated macrophages promote ovarian cancer cells induced-angiogenesis

Recently, tumor-associated macrophages in the cancer microenvironment become a hot topic in cancer research. Macrophages are innate immune cells with high plasticity, and their heterogeneity depends on different cytokine stimulation at specific location^{24,27,44,52}. Many clinical and experimental data have described the existence of various macrophage sub-types. Tumor-associated macrophages with the M2-subtype are shown to polarize from the Th2 cytokines stimulation^{24,27}. The tumor-associated macrophages reported in early cancer research were mainly prepared from human peripheral blood mononuclear cells or from the mouse model^{32,53}. Tjiu's group in 2009 has developed a quick and easy protocol to induce THP-1 to differentiate into different macrophage subsets *in vitro*³⁹. This proven method enables generation of the M2-polarized macrophages for various experiments. In this study, I followed Tjiu's protocol to polarize THP-1 cells into M2-polarized macrophages, and confirmed the cells' marker genes expression profile with real-time PCR (Fig. 8). Although there are still difference between the native tumor-associated macrophages and the M2-polarized macrophages, they are still a powerful tool and materials for my study.

After co-cultured with M2-polarized macrophages, the dramatic increase of VEGFA and cathepsin S gene expression in SKOV3 cells *in vitro* suggest TAMs could play a significant role in ovarian cancer-induced angiogenesis *in vivo*. Our *in vitro* data also revealed the paracrine

interaction between macrophages and cancer cells were critical in the induction of angiogenesis-related gene expression. So far, VEGFA has been reported to be secreted by many cancer cells and has been shown to play a coordinated role in promoting malignant tumor growth and migration with helps from the surrounding tumor-associated macrophages^{18,39,45}. My real-time PCR data indicate that VEGFA gene expression profile in SKOV3 co-cultured with M2 macrophages was also consistent with previous studies in human patients or other animal models³⁹. Meanwhile, cysteine cathepsins are found to be highly expressed in malignant tissues^{37,54}. Cathepsin B and S have been shown to exhibit high enzyme activities within tumor-associated macrophages in pancreatic tumor^{32,55}. In my study, I found cathepsin S is increased in the ovarian cancer cells after co-cultured with macrophages. To my knowledge, my study is the first to reveal the cathepsin S expression and enzymatic activity in ovarian cancer would be increased after paracrine stimulation by tumor-associated macrophages, and the enhanced cathepsin S production was in addition to the ones produced by the TAMs as reported by other studies³². My results showed that the M2-polarized macrophages could trigger the angiogenesis-related gene expression in ovarian cancer cells.

Because the *in vitro* assay system and analysis could not represent the complex tumor microenvironment, here I developed and used the zebrafish tumor xenograft model to investigate the angiogenesis induced by the interaction between tumor cells and macrophages in microenvironment. I co-injected the SKOV3 cells and M2-polarized macrophages into a single zebrafish embryo with fluorescent endothelial cells. When co-injected with macrophages, the degree of SKOV3-induced angiogenesis was significantly increased. This result revealed the macrophages indeed play a critical role in tumor-induced angiogenesis.

In conclusion, my *in vitro* and *in vivo* assay systems provide insight into the complex interaction between ovarian cancer cells and macrophages in a living tumor microenvironment. My findings may pave the basis to develop drug to target TAM-dependent cathepsin production or activity to block tumor-induced angiogenesis in ovarian cancer therapy.

5. Reference:

1. Baeriswyl, V. & Christofori, G. The angiogenic switch in carcinogenesis. *Semin Cancer Biol* **19**, 329-337 (2009).
2. Spannuth, W.A., Sood, A.K. & Coleman, R.L. Angiogenesis as a strategic target for ovarian cancer therapy. *Nat Clin Pract Oncol* **5**, 194-204 (2008).
3. Nussenbaum, F. & Herman, I.M. Tumor angiogenesis: insights and innovations. *J Oncol* **2010**, 132641 (2010).
4. Staton, C.A., Reed, M.W. & Brown, N.J. A critical analysis of current in vitro and in vivo angiogenesis assays. *Int J Exp Pathol* **90**, 195-221 (2009).
5. Staton, C.A., Stribbling, S. M., Tazzyman, S., Hughes, R., Brown, N. J. & Lewis, C. E. Current methods for assaying angiogenesis in vitro and in vivo. *Int J Exp Pathol* **85**, 233-248 (2004).
6. Nicoli, S., Ribatti, D., Cotelli, F. & Presta, M. Mammalian tumor xenografts induce neovascularization in zebrafish embryos. *Cancer Res* **67**, 2927-2931 (2007).
7. Serbedzija, G.N., Flynn, E. & Willett, C.E. Zebrafish angiogenesis: a new model for drug screening. *Angiogenesis* **3**, 353-359 (1999).
8. Lee, S.L., Rouhi, P., Dahl Jensen, L., Zhang, D., Ji, H., Hauptmann, G., Ingham, P. & Cao, Y. Hypoxia-induced pathological angiogenesis mediates tumor cell dissemination, invasion, and metastasis in a zebrafish tumor model. *Proc Natl Acad Sci U S A* **106**, 19485-19490 (2009).
9. Marques, I.J., Weiss, F. U., Vlecken, D. H., Nitsche, C., Bakkers, J., Lagendijk, A. K., Partecke, L. I., Heidecke, C. D., Lerch, M. M. & Bagowski, C. P. Metastatic behaviour of primary human tumours in a zebrafish xenotransplantation model. *BMC Cancer* **9**, 128 (2009).
10. Nicoli, S. & Presta, M. The zebrafish/tumor xenograft angiogenesis assay. *Nat Protoc* **2**, 2918-2923 (2007).
11. Stoletov, K. & Klemke, R. Catch of the day: zebrafish as a human cancer model. *Oncogene* **27**, 4509-4520 (2008).
12. Freedman, R.S., Ma, Q., Wang, E., Gallardo, S. T., Gordon, I. O., Shin, J. W., Jin, P., Stroncek, D. & Marincola, F. M. Migration deficit in monocyte-macrophages in human ovarian cancer. *Cancer Immunol Immunother* **57**, 635-645 (2008).
13. Jeon, B.H., Jang, C., Han, J., Kataru, R. P., Piao, L., Jung, K., Cha, H. J., Schwendener, R. A., Jang, K. Y., Kim, K. S., Alitalo, K. & Koh, G. Y. Profound but dysfunctional lymphangiogenesis via vascular endothelial growth factor ligands from CD11b+ macrophages in advanced ovarian cancer. *Cancer Res* **68**, 1100-1109 (2008).
14. Luo, J.C., Yamaguchi, S., Shinkai, A., Shitara, K. & Shibuya, M. Significant expression of vascular endothelial growth factor/vascular permeability factor in mouse ascites tumors. *Cancer Res* **58**, 2652-2660 (1998).
15. Coffelt, S.B., Hughes, R. & Lewis, C.E. Tumor-associated macrophages: effectors of angiogenesis and tumor progression. *Biochim Biophys Acta* **1796**, 11-18 (2009).

16. Lamagna, C., Aurrand-Lions, M. & Imhof, B.A. Dual role of macrophages in tumor growth and angiogenesis. *J Leukoc Biol* **80**, 705-713 (2006).
17. Condeelis, J. & Pollard, J.W. Macrophages: obligate partners for tumor cell migration, invasion, and metastasis. *Cell* **124**, 263-266 (2006).
18. Luo, Y., Zhou, H., Krueger, J., Kaplan, C., Lee, S. H., Dolman, C., Markowitz, D., Wu, W., Liu, C., Reisfeld, R. A. & Xiang, R. Targeting tumor-associated macrophages as a novel strategy against breast cancer. *J Clin Invest* **116**, 2132-2141 (2006).
19. Mantovani, A., Sica, A., Sozzani, S., Allavena, P., Vecchi, A. & Locati, M. The chemokine system in diverse forms of macrophage activation and polarization. *Trends Immunol* **25**, 677-686 (2004).
20. Pollard, J.W. Tumour-educated macrophages promote tumour progression and metastasis. *Nat Rev Cancer* **4**, 71-78 (2004).
21. Kawamura, K., Komohara, Y., Takaishi, K., Katabuchi, H. & Takeya, M. Detection of M2 macrophages and colony-stimulating factor 1 expression in serous and mucinous ovarian epithelial tumors. *Pathol Int* **59**, 300-305 (2009).
22. Kurahara, H., Shinchu, H., Mataka, Y., Maemura, K., Noma, H., Kubo, F., Sakoda, M., Ueno, S., Natsugoe, S. & Takao, S. Significance of M2-Polarized Tumor-Associated Macrophage in Pancreatic Cancer. *J Surg Res* (2009).
23. O'Brien, J. & Schedin, P. Macrophages in breast cancer: do involution macrophages account for the poor prognosis of pregnancy-associated breast cancer? *J Mammary Gland Biol Neoplasia* **14**, 145-157 (2009).
24. Gordon, S. & Martinez, F.O. Alternative activation of macrophages: mechanism and functions. *Immunity* **32**, 593-604 (2010).
25. Mantovani, A., Sozzani, S., Locati, M., Allavena, P. & Sica, A. Macrophage polarization: tumor-associated macrophages as a paradigm for polarized M2 mononuclear phagocytes. *Trends Immunol* **23**, 549-555 (2002).
26. Mantovani, A. & Sica, A. Macrophages, innate immunity and cancer: balance, tolerance, and diversity. *Curr Opin Immunol* **22**, 231-237 (2010).
27. Qian, B.Z. & Pollard, J.W. Macrophage diversity enhances tumor progression and metastasis. *Cell* **141**, 39-51 (2010).
28. Carpini, J.D., Karam, A.K. & Montgomery, L. Vascular endothelial growth factor and its relationship to the prognosis and treatment of breast, ovarian, and cervical cancer. *Angiogenesis* **13**, 43-58 (2010).
29. Paley, P.J., Goff, B.A., Gown, A.M., Greer, B.E. & Sage, E.H. Alterations in SPARC and VEGF immunoreactivity in epithelial ovarian cancer. *Gynecol Oncol* **78**, 336-341 (2000).
30. Yoneda, J., Kuniyasu, H., Crispens, M. A., Price, J. E., Bucana, C. D. & Fidler, I. J. Expression of angiogenesis-related genes and progression of human ovarian carcinomas in nude mice. *J Natl Cancer Inst* **90**, 447-454 (1998).
31. Weis, S.M. & Cheresh, D.A. Pathophysiological consequences of VEGF-induced vascular

- permeability. *Nature* **437**, 497-504 (2005).
32. Gocheva, V., Wang, H. W., Gadea, B. B., Shree, T., Hunter, K. E., Garfall, A. L., Berman, T. & Joyce, J. A. IL-4 induces cathepsin protease activity in tumor-associated macrophages to promote cancer growth and invasion. *Genes Dev* **24**, 241-255 (2010).
 33. Joyce, J.A., Baruch, A., Chehade, K., Meyer-Morse, N., Giraudo, E., Tsai, F. Y., Greenbaum, D. C., Hager, J. H., Bogyo, M. & Hanahan, D. Cathepsin cysteine proteases are effectors of invasive growth and angiogenesis during multistage tumorigenesis. *Cancer Cell* **5**, 443-453 (2004).
 34. Hazen, L.G., Bleeker, F. E., Lauritzen, B., Bahns, S., Song, J., Jonker, A., Van Driel, B. E., Lyon, H., Hansen, U., Kohler, A. & Van Noorden, C. J. Comparative localization of cathepsin B protein and activity in colorectal cancer. *J Histochem Cytochem* **48**, 1421-1430 (2000).
 35. Kos, J., Sekirnik, A., Kopitar, G., Cimerman, N., Kayser, K., Stremmer, A., Fiehn, W. & Werle, B. Cathepsin S in tumours, regional lymph nodes and sera of patients with lung cancer: relation to prognosis. *Br J Cancer* **85**, 1193-1200 (2001).
 36. Koblinski, J.E., Dosescu, J., Sameni, M., Moin, K., Clark, K. & Sloane, B. F. Interaction of human breast fibroblasts with collagen I increases secretion of procathepsin B. *J Biol Chem* **277**, 32220-32227 (2002).
 37. Mohamed, M.M. & Sloane, B.F. Cysteine cathepsins: multifunctional enzymes in cancer. *Nat Rev Cancer* **6**, 764-775 (2006).
 38. Rao, J.S. Molecular mechanisms of glioma invasiveness: the role of proteases. *Nat Rev Cancer* **3**, 489-501 (2003).
 39. Tjiu, J.W., Chen, J. S., Shun, C. T., Lin, S. J., Liao, Y. H., Chu, C. Y., Tsai, T. F., Chiu, H. C., Dai, Y. S., Inoue, H., Yang, P. C., Kuo, M. L. & Jee, S. H. Tumor-associated macrophage-induced invasion and angiogenesis of human basal cell carcinoma cells by cyclooxygenase-2 induction. *J Invest Dermatol* **129**, 1016-1025 (2009).
 40. Honig, M.G. & Hume, R.I. Fluorescent carbocyanine dyes allow living neurons of identified origin to be studied in long-term cultures. *J Cell Biol* **103**, 171-187 (1986).
 41. Kuffler, D.P. Long-term survival and sprouting in culture by motoneurons isolated from the spinal cord of adult frogs. *J Comp Neurol* **302**, 729-738 (1990).
 42. Hall, C., Flores, M.V., Storm, T., Crosier, K. & Crosier, P. The zebrafish lysozyme C promoter drives myeloid-specific expression in transgenic fish. *BMC Dev Biol* **7**, 42 (2007).
 43. Liu, F. & Wen, Z. Cloning and expression pattern of the lysozyme C gene in zebrafish. *Mech Dev* **113**, 69-72 (2002).
 44. Stout, R.D., Watkins, S.K. & Suttles, J. Functional plasticity of macrophages: in situ reprogramming of tumor-associated macrophages. *J Leukoc Biol* **86**, 1105-1109 (2009).
 45. Halin, S., Rudolfsson, S.H., Van Rooijen, N. & Bergh, A. Extratumoral macrophages promote tumor and vascular growth in an orthotopic rat prostate tumor model. *Neoplasia* **11**, 177-186 (2009).
 46. Pierson, R.N., 3rd, Winn, H.J., Russell, P.S. & Auchincloss, H., Jr. Xenogeneic skin graft

- rejection is especially dependent on CD4+ T cells. *J Exp Med* **170**, 991-996 (1989).
47. Schmidt, P., Krook, H., Maeda, A., Korsgren, O. & Benda, B. A new murine model of islet xenograft rejection: graft destruction is dependent on a major histocompatibility-specific interaction between T-cells and macrophages. *Diabetes* **52**, 1111-1118 (2003).
 48. Lam, S.H., Chua, H.L., Gong, Z., Lam, T.J. & Sin, Y.M. Development and maturation of the immune system in zebrafish, *Danio rerio*: a gene expression profiling, in situ hybridization and immunological study. *Dev Comp Immunol* **28**, 9-28 (2004).
 49. Davidson, A.J. & Zon, L.I. The 'definitive' (and 'primitive') guide to zebrafish hematopoiesis. *Oncogene* **23**, 7233-7246 (2004).
 50. Fox, A., Mountford, J., Braakhuis, A. & Harrison, L.C. Innate and adaptive immune responses to nonvascular xenografts: evidence that macrophages are direct effectors of xenograft rejection. *J Immunol* **166**, 2133-2140 (2001).
 51. Herbolme, P., Thisse, B. & Thisse, C. Ontogeny and behaviour of early macrophages in the zebrafish embryo. *Development* **126**, 3735-3745 (1999).
 52. Mantovani, A., Sica, A., Allavena, P., Garlanda, C. & Locati, M. Tumor-associated macrophages and the related myeloid-derived suppressor cells as a paradigm of the diversity of macrophage activation. *Hum Immunol* **70**, 325-330 (2009).
 53. Duluc, D., Delneste, Y., Tan, F., Moles, M. P., Grimaud, L., Lenoir, J., Preisser, L., Anegón, I., Catala, L., Ifrah, N., Descamps, P., Gamelin, E., Gascan, H., Hebbard, M. & Jeannin, P. Tumor-associated leukemia inhibitory factor and IL-6 skew monocyte differentiation into tumor-associated macrophage-like cells. *Blood* **110**, 4319-4330 (2007).
 54. Wang, B., Sun, J., Kitamoto, S., Yang, M., Grubb, A., Chapman, H. A., Kalluri, R. & Shi, G. P. Cathepsin S controls angiogenesis and tumor growth via matrix-derived angiogenic factors. *J Biol Chem* **281**, 6020-6029 (2006).
 55. Gocheva, V., Zeng, W., Ke, D., Klimstra, D., Reinheckel, T., Peters, C., Hanahan, D. & Joyce, J. A. Distinct roles for cysteine cathepsin genes in multistage tumorigenesis. *Genes Dev* **20**, 543-556 (2006).

Table 1. The sequence of primers used for real-time quantitative PCR

Gene name	Forward (5'-3')	Reverse (5'-3')	Amplicon length (base-pair)
MRC1	GCGTCTTCTGGGTTTTGGAG	ATGACTACTCCGGCCACGTT	170
SR1	TGACTTTGGTTCCCGTGTTG	CGTGCATGAGAGGTGTCCAG	163
TNF	CTCACTGGGGCCTACAGCTT	GGCTCCGTGTCTCAAGGAAG	174
IL6	TGCAATAACCACCCCTGACC	GGAATGCCCATTAACAACAACA	192
IL12B	CTTGTGGTCCCAGCTGTTCA	AGAGAGGTGGGGGTGAGGAC	170
VEGFA	GGACTCGCCCTCATCCTCTT	TGGATCCTGCCCTGTCTCTC	193
CTSB	GCAGTGAGCCAAGACAGTGC	TGCCAAGGCTGATCTCAAAA	188
CTSS	CCTTCTGCCTGCTGTTCTCC	TTCCTCTTTGTGTCCCTGTGC	163
GAPDH	TTGTGATGGGTGTGAACCAC	GGATGCAGGGATGATGTTCT	239

GAPDH is the endogenous control in our real-time PCR assay.

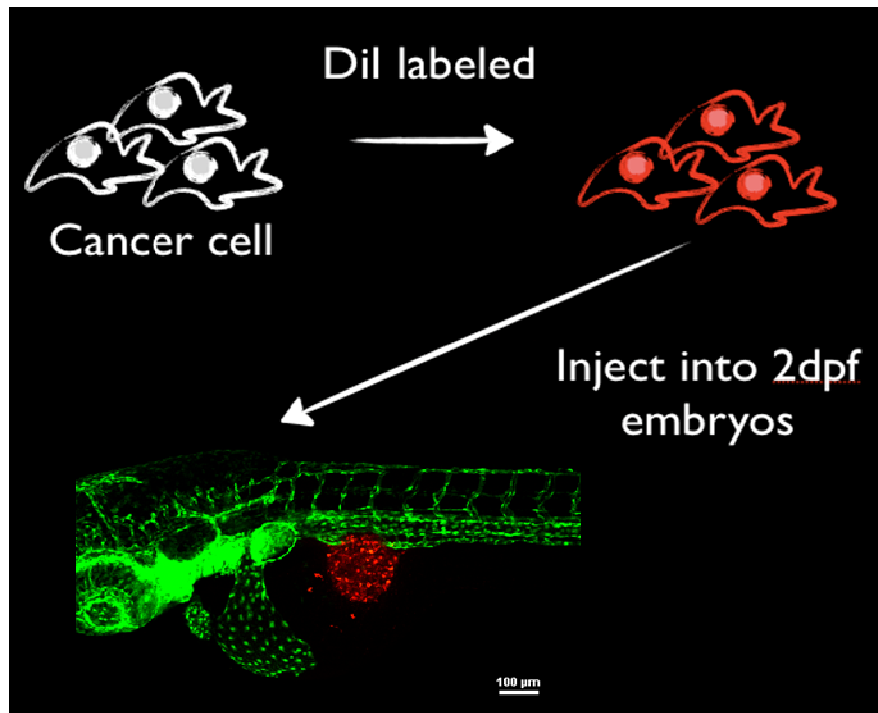


Figure 1. Zebrafish tumor xenograft model

The cancer cells were labeled with 3.75 $\mu\text{g/ml}$ Dil. Approximately 400 cancer cells suspended in 4.6 nl matrigel (10 $\mu\text{g/ml}$) were implanted into the perivitelline space of 2 days post-fertilization (dpf) *Tg(kdr:EGFP)* zebrafish embryos. Cancer cells and the zebrafish vessels were monitored using the Nikon A1R real-time confocal microscopy at different time point. Color code: Fish blood vessels are green, and human tumor cells are red.

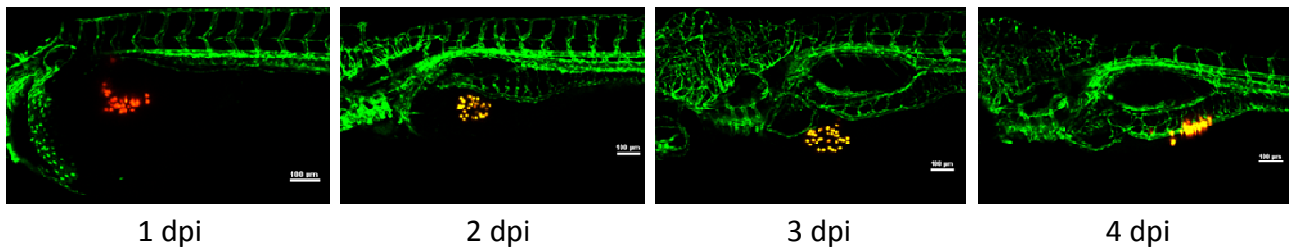
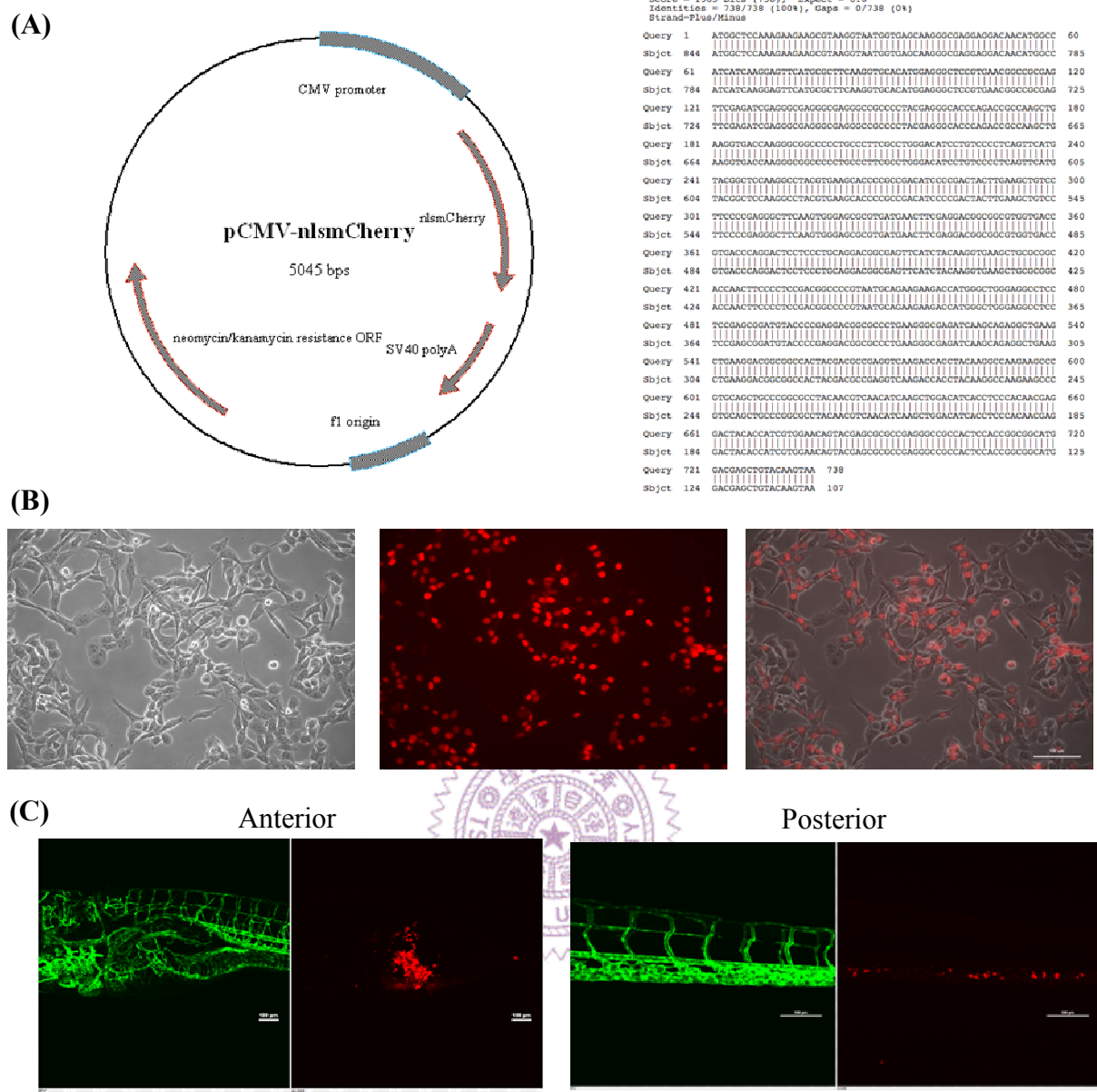


Figure 2. The control microspheres did not migrate or induce angiogenesis in zebrafish

Red fluorescent microspheres (10 µm diameter) were suspended in the 9.6 mg/ml matrigel and injected into 2 dpf zebrafish embryos, and monitored by real-time confocal microscope in following days. (Scale bar, 100 µm.) Color code: Fish blood vessels are green, and microspheres are red.





Score = 1363 bits (738), Expect = 0.0
Identities = 738/738 (100%), Gaps = 0/738 (0%)
Strand=Plus/Minus

Query	1	ATGGCTCCAAAGAGAGCCGTAAGGTATGTTAGCAAGGCCGAGGAGCAACATGGCC	60
Sbjct	844	ATGGCTCCAAAGAGAGCCGTAAGGTATGTTAGCAAGGCCGAGGAGCAACATGGCC	785
Query	61	ATCATCAAGGAGTTGATGGCTTCAAGGTGACATGAGGGCTCCCTGAAGGCCGAG	120
Sbjct	784	ATCATCAAGGAGTTGATGGCTTCAAGGTGACATGAGGGCTCCCTGAAGGCCGAG	725
Query	121	TTCCGAGATCGAGGGCGGCGGCGGCGGCGGCGGCGGCGGCGGCGGCGGCGGCGG	180
Sbjct	724	TTCCGAGATCGAGGGCGGCGGCGGCGGCGGCGGCGGCGGCGGCGGCGGCGGCGG	645
Query	181	AGGTGACCAAGGGCGGCGGCGGCGGCGGCGGCGGCGGCGGCGGCGGCGGCGG	240
Sbjct	654	AGGTGACCAAGGGCGGCGGCGGCGGCGGCGGCGGCGGCGGCGGCGGCGGCGG	605
Query	241	TACGGCTCCAGGGCTAGGTGAGGACGCGGCGGCGGCGGCGGCGGCGGCGGCGG	300
Sbjct	604	TACGGCTCCAGGGCTAGGTGAGGACGCGGCGGCGGCGGCGGCGGCGGCGGCGG	545
Query	301	TTCCCGGAGGGCTCAAGTGGGAGCGGCGGCGGCGGCGGCGGCGGCGGCGGCGG	360
Sbjct	544	TTCCCGGAGGGCTCAAGTGGGAGCGGCGGCGGCGGCGGCGGCGGCGGCGGCGG	485
Query	361	GTGACCGAGGACTCCCTCCGCGAGGACGCGGCGGCGGCGGCGGCGGCGGCGG	420
Sbjct	484	GTGACCGAGGACTCCCTCCGCGAGGACGCGGCGGCGGCGGCGGCGGCGGCGG	425
Query	421	ACCAACTTCCCTCCGCGAGGCGGCGGCGGCGGCGGCGGCGGCGGCGGCGGCGG	480
Sbjct	424	ACCAACTTCCCTCCGCGAGGCGGCGGCGGCGGCGGCGGCGGCGGCGGCGGCGG	365
Query	481	TTCCGAGCGGATGATCCCGGAGGCGGCGGCGGCGGCGGCGGCGGCGGCGGCGG	540
Sbjct	364	TTCCGAGCGGATGATCCCGGAGGCGGCGGCGGCGGCGGCGGCGGCGGCGGCGG	305
Query	541	CTGAGGACCGGCGGCGGCGGCGGCGGCGGCGGCGGCGGCGGCGGCGGCGGCGG	600
Sbjct	304	CTGAGGACCGGCGGCGGCGGCGGCGGCGGCGGCGGCGGCGGCGGCGGCGGCGG	245
Query	601	GTCCAGCTGCGGCGGCGGCGGCGGCGGCGGCGGCGGCGGCGGCGGCGGCGGCGG	660
Sbjct	244	GTCCAGCTGCGGCGGCGGCGGCGGCGGCGGCGGCGGCGGCGGCGGCGGCGGCGG	185
Query	661	GACTACACCATCTGGAGACGTTAGGAGCGGCGGCGGCGGCGGCGGCGGCGGCGG	720
Sbjct	184	GACTACACCATCTGGAGACGTTAGGAGCGGCGGCGGCGGCGGCGGCGGCGGCGG	125
Query	721	GACGAGCTGTACAGTAA 738	
Sbjct	124	GACGAGCTGTACAGTAA 107	

Figure 3. CL1-5 with endogenous nuclear mCherry indicated human cancer cells could survive and migrate in zebrafish

(A) Construction of pCMV-nlsmCherry plasmid. The pCMV-nlsmCherry plasmid was sequence verified by multiple sequences alignment. (B) The image of stable nlsmCherry expressed CL1-5 cells which selected by G418 antibiotic. Red: nuclear-localized mCherry. (C) nlsmCherry-labeled CL1-5 cells were injected into 2 dpf zebrafish embryo. (Scale bar, 100 μ m.) Color code: Fish blood vessels are green, and nlsmCherry-labeled CL1-5 cells are red.

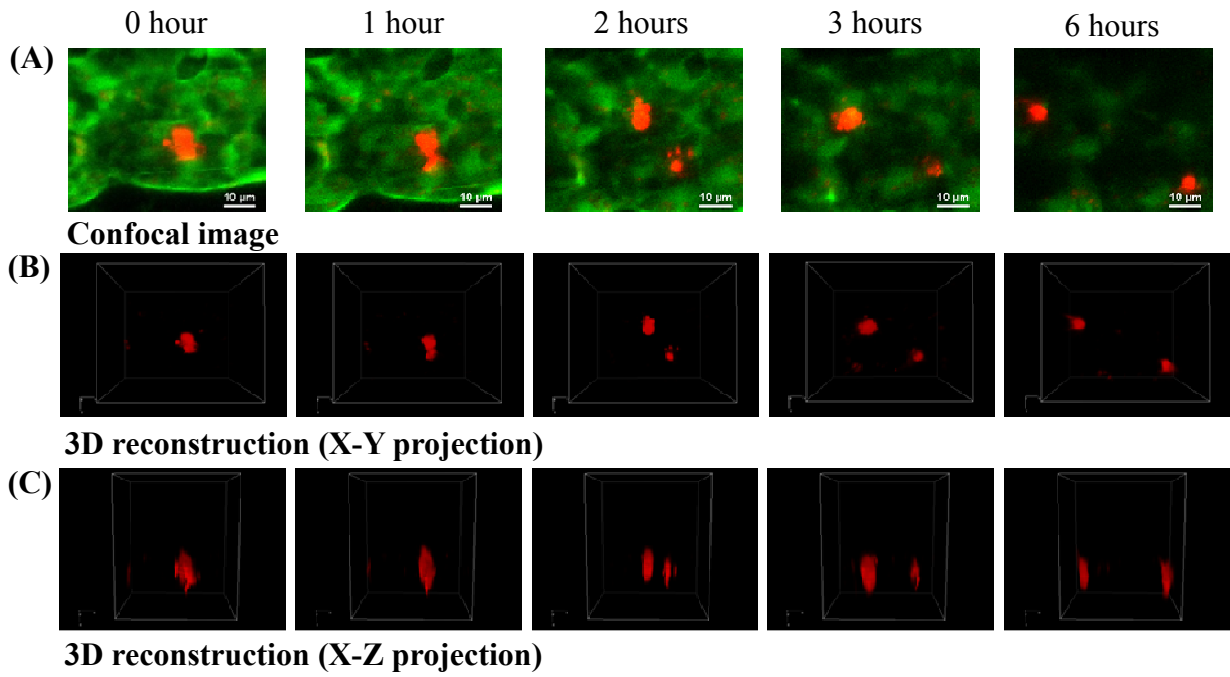


Figure 4. Cancer cell mitosis in zebrafish

DiI-labeled CL1-5 cells were injected into 2 dpf zebrafish embryos. At the posterior region of the embryos, the cell mitosis can be traced with real-time images by the A1R confocal microscopy. (A) Confocal images and (B) (C) 3D reconstruction images of the X-Y projection and X-Z projection. Color code: Fish blood vessels are green, and DiI-labeled CL1-5 cells are red.

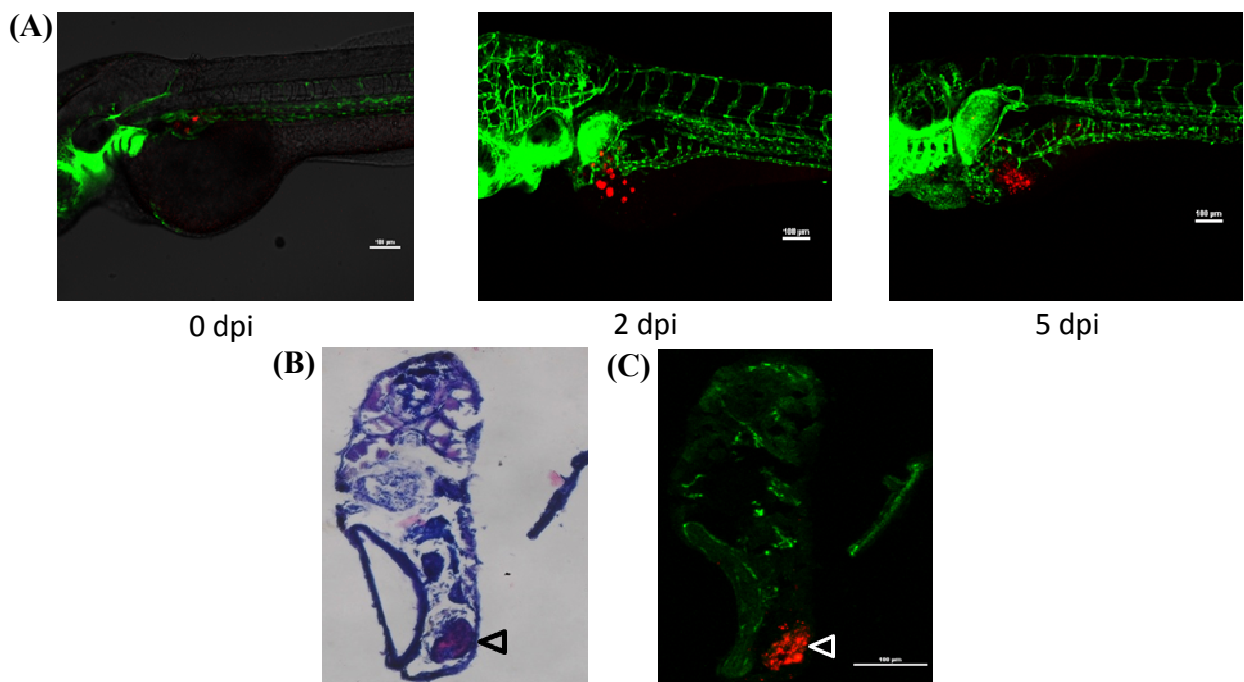


Figure 5. Cancer cell mass was formed at the perivitelline space

Melanoma cells (A2058) were injected into perivitelline space in the presence of 9.6 mg/ml matrigel. Approximately 20 cells of A2058 were injected into the 2 dpf zebrafish embryos. (A) DiI-labeled tumor cells were monitored by confocal microscopy on days 0, 2 and 5 post-injection. (B, C) Cryosection of 5 dpi zebrafish embryos show the cell mass of A2058 (arrowhead) at the perivitelline space. (HE staining in B and confocal image in C) (Scale bar, 100 μm.) Color code: Fish blood vessels are green, and DiI-labeled A2058 cells are red.

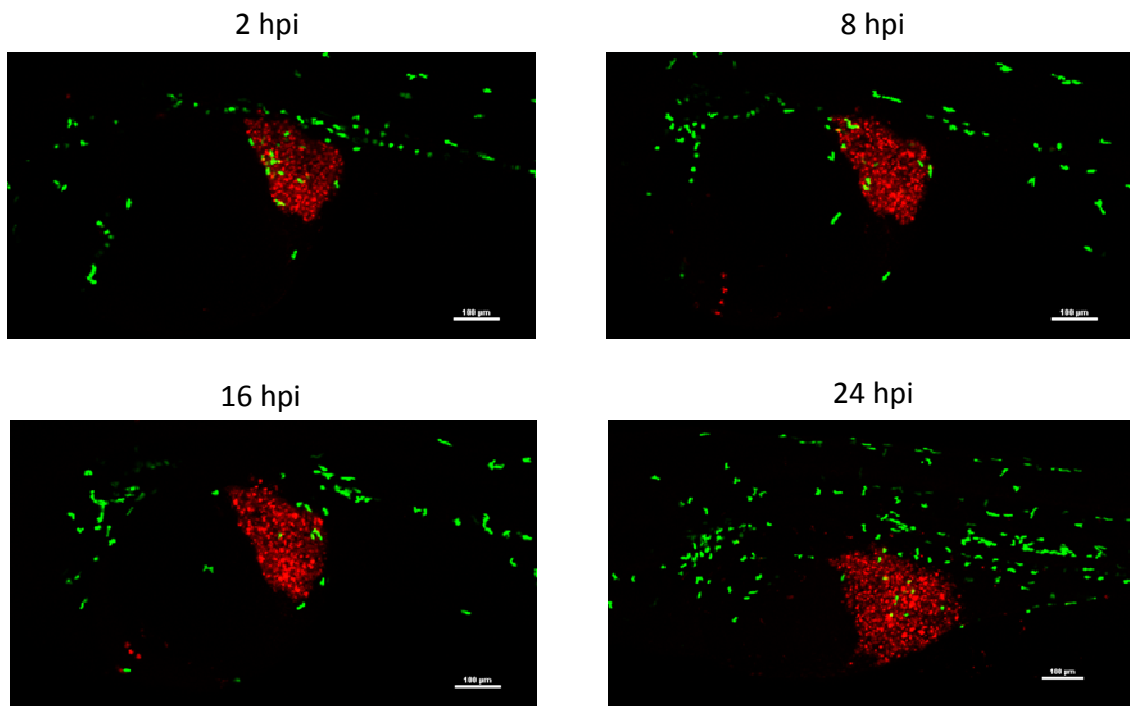


Figure 6. No cancer-host immune cell interaction was observed around the tumor xenograft

DiI-labeled CL1-5 cells were injected into 2 dpf Tg (*lyz:EGFP*) zebrafish embryos. The macrophages of zebrafish and cancer cells were traced by confocal microscopy for 24 hours. (Scale bar, 100 μm.) Color code: Fish macrophages are green, and DiI-labeled CL1-5 cells are red.

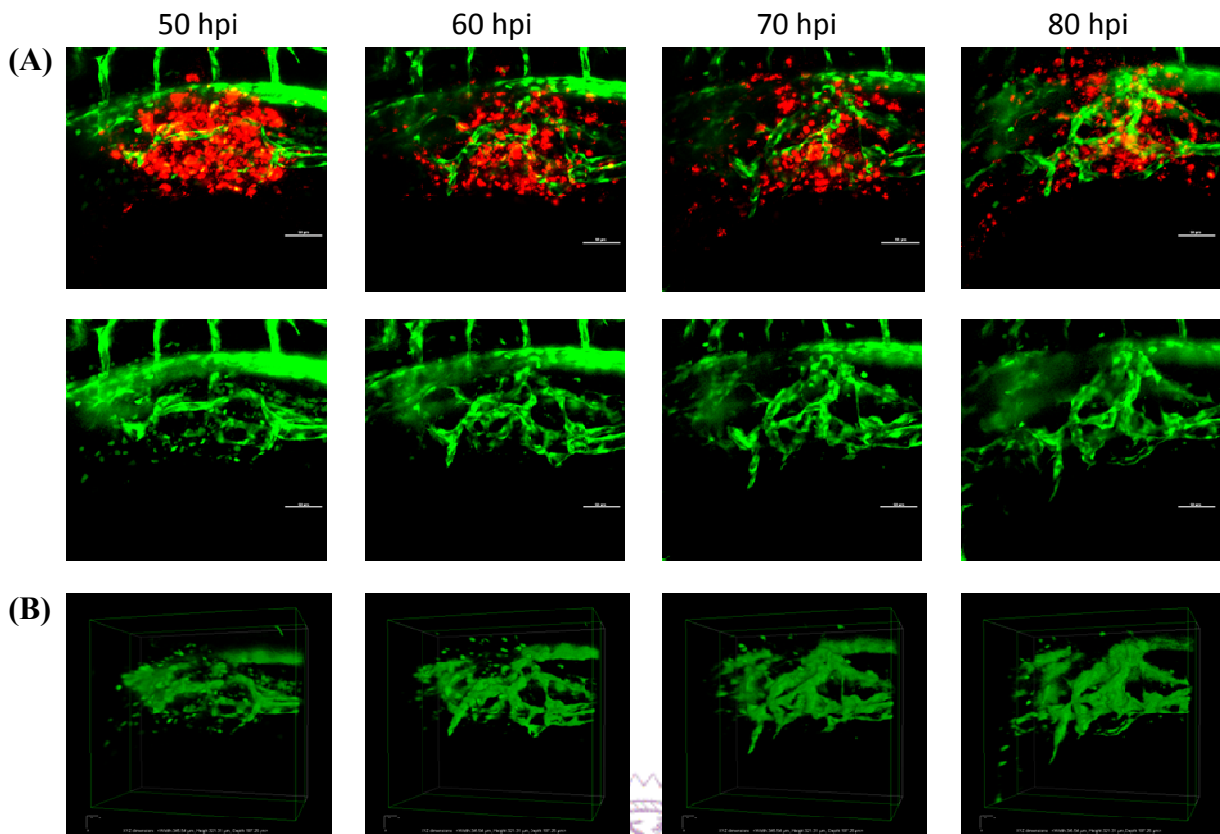


Figure 7. The dynamic process of tumor-induced angiogenesis was monitored for up to 80 hours

DiI-labeled CL1-5 cells were injected into the perivitelline space of 2 dpf zebrafish embryos. (A) The tumor-induced angiogenesis of the sub-intestinal vessels were monitored for 30 hours in two days post-injection zebrafish embryos by the real-time A1R confocal microscopy. (Scale bar, 50 μm .) (B) Three-dimensional reconstruction of tumor-induced angiogenesis in cancer cell mass was shown. Color code: Fish blood vessels are green, and DiI-labeled CL1-5 cells are red.

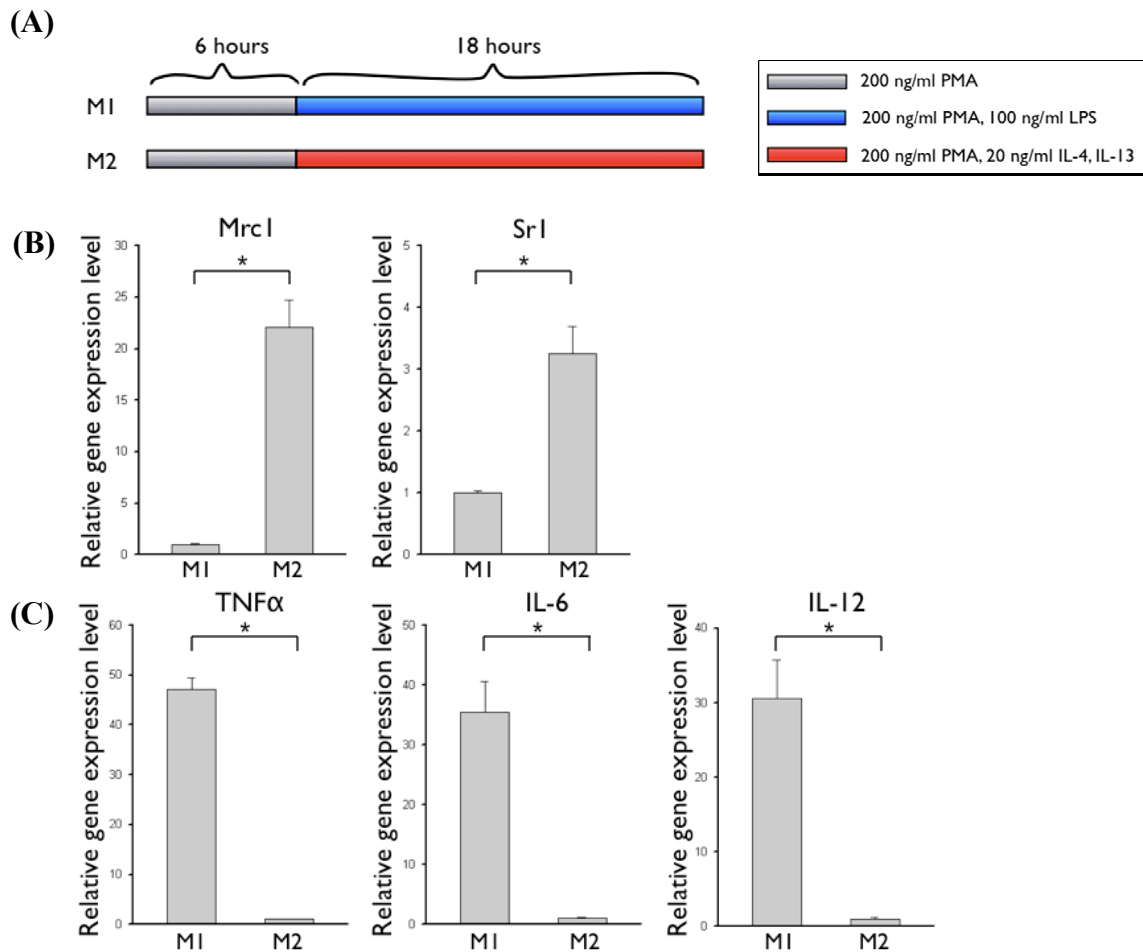


Figure 8. THP-1 cells were polarized into the M2 macrophages

THP-1 cells were exposed to Th1 or Th2 cytokine and polarized into different subtypes of macrophages. (A) The schema THP-1 cells polarized into M1 and M2-phenotype macrophages. THP-1 cells were treated with 200 ng/ml PMA for 6 hours and 100 ng/ml LPS for the following 18 hours to M1-polarized macrophages; and THP-1 cells were treated with 200 ng/ml PMA for 6 hours and 20 ng/ml IL-4 and IL-13 for the following 18 hours to M2-polarized macrophages. (B) (C) M2-polarized macrophages were examined the M2 marker genes in (B) and M1 marker genes in (C) to confirm the phenotype. In M2-polarized macrophages, mannose receptor (Mrc 1) increased 21.688-fold and scavenger receptor (Sr 1) increased 3.251-fold than M1-polarized macrophages. TNF- α decreased 46.971-fold, IL-6 decreased 35.216-fold and IL-12 decreased 30.218-fold in M2-polarized macrophages. (*, $P < 0.01$) (n=3)

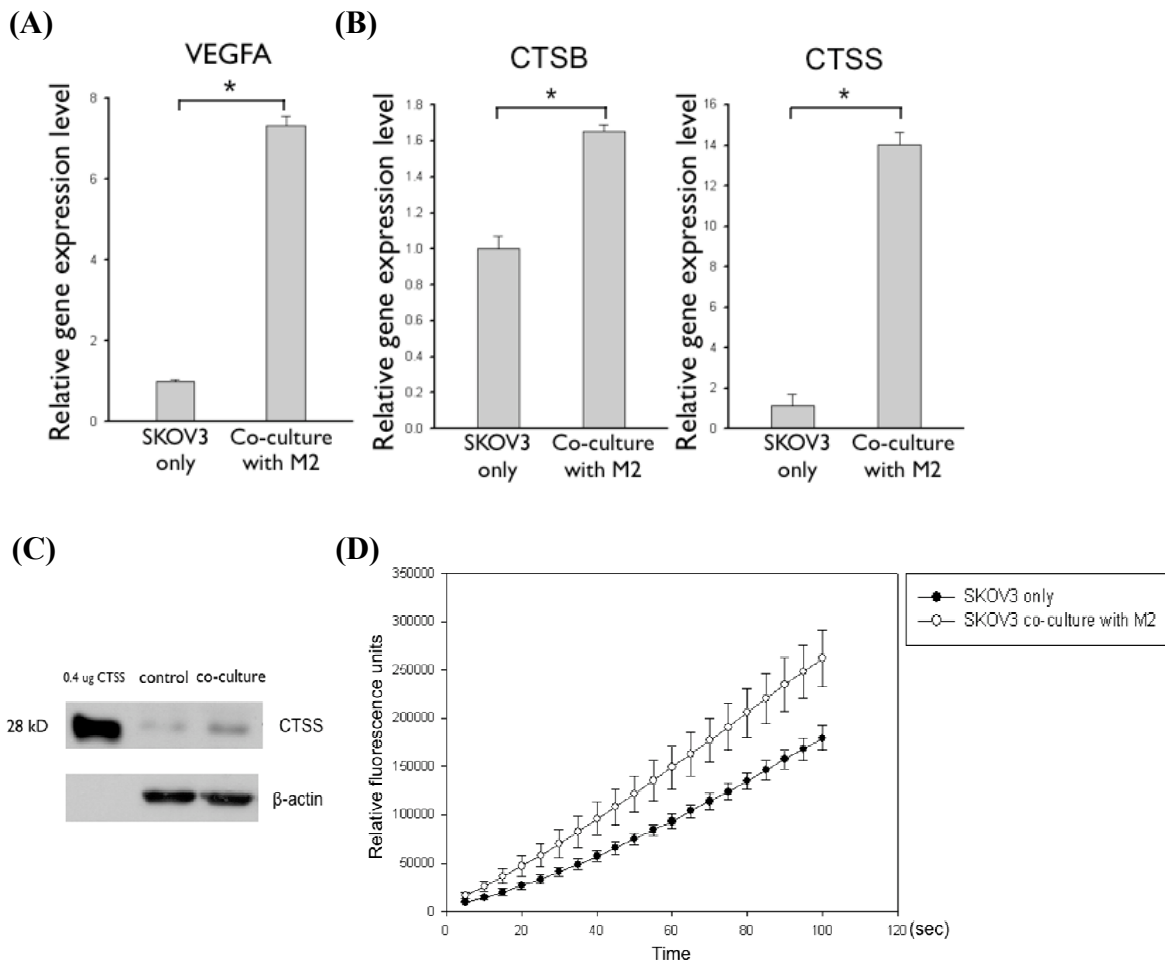


Figure 9. Expression level of CTSS was increased in SKOV3 cells co-cultured with polarized M2 macrophages

(A) (B) After co-cultured with polarized M2 macrophages for 6 hours, the RNA of SKOV3 were harvested and examined VEGFA and cathepsin B and S gene expression. VEGFA increased 7.324-fold, cathepsin B increased 1.648-fold and cathepsin S increased 12.549-fold, compared with control group. (*, $P < 0.01$) ($n = 3$) (C) The protein level of cathepsin S in SKOV3 cells was examined after co-cultured with M2-polarized macrophages for 48 hours. (D) The cathepsin S kinetic activity was analysis by add Z-VVR-AMC, the specific substrate of cathepsin S. The relative fluorescence units represent the concentration of the product.

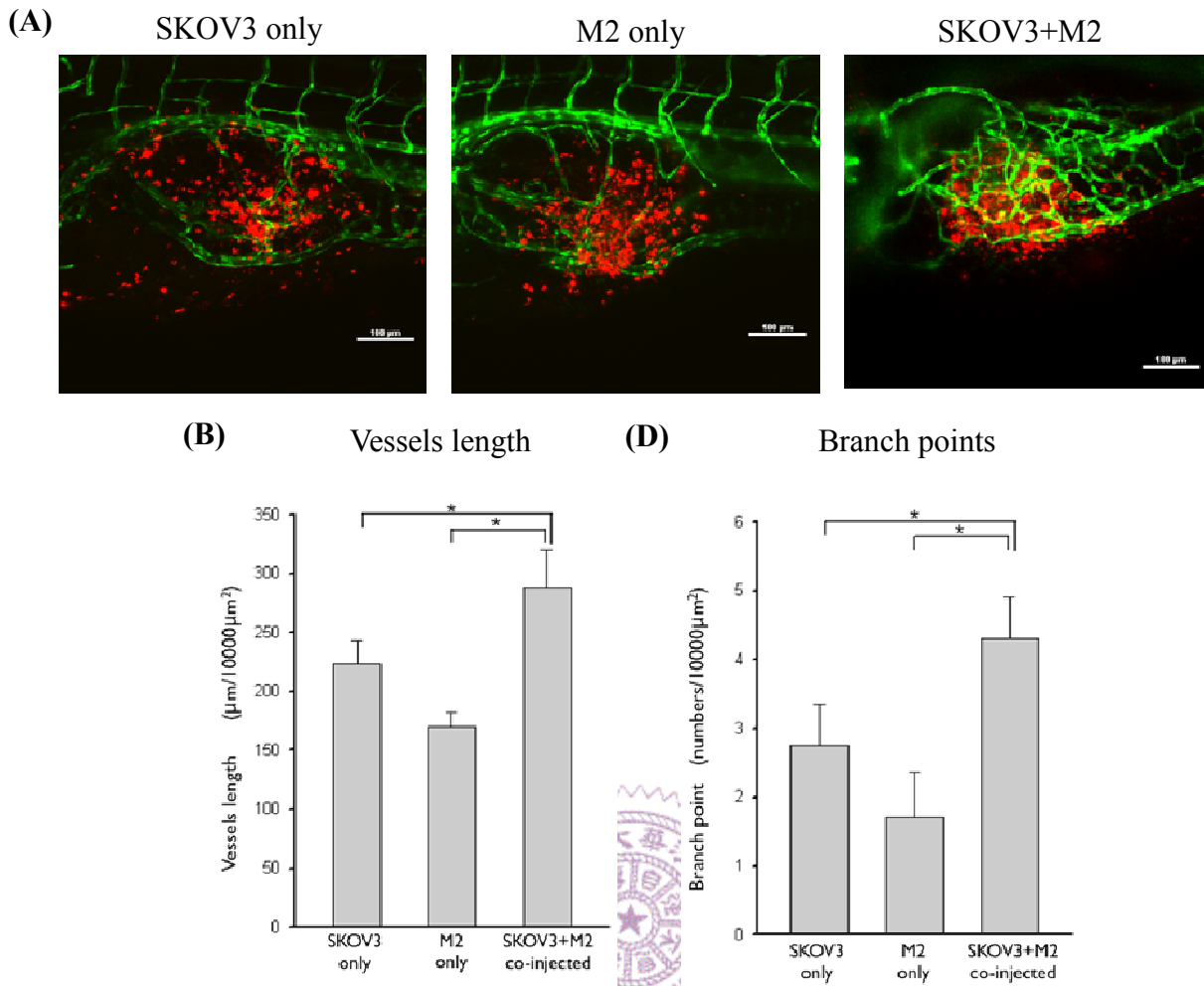


Figure 10. Polarized M2 macrophages effectively promoted SKOV3 cells to induce

angiogenesis

M2-polarized macrophages were co-injected with DiI-labeled SKOV3 cells into 2 dpf zebrafish embryos. (A) The tumor-induced angiogenesis were examined by confocal microscope. (Scale bar, 100 μm.) (B) Quantification of the length of vessels related to tumor area. (C) Quantification of the branch point of vessels related to tumor area. The total vessels length and branch points increased 1.3-fold and 1.6-fold respectively after co-injected M2-polarized macrophages (*, $P < 0.01$) ($n = 6$) Data are represented as mean \pm SD.

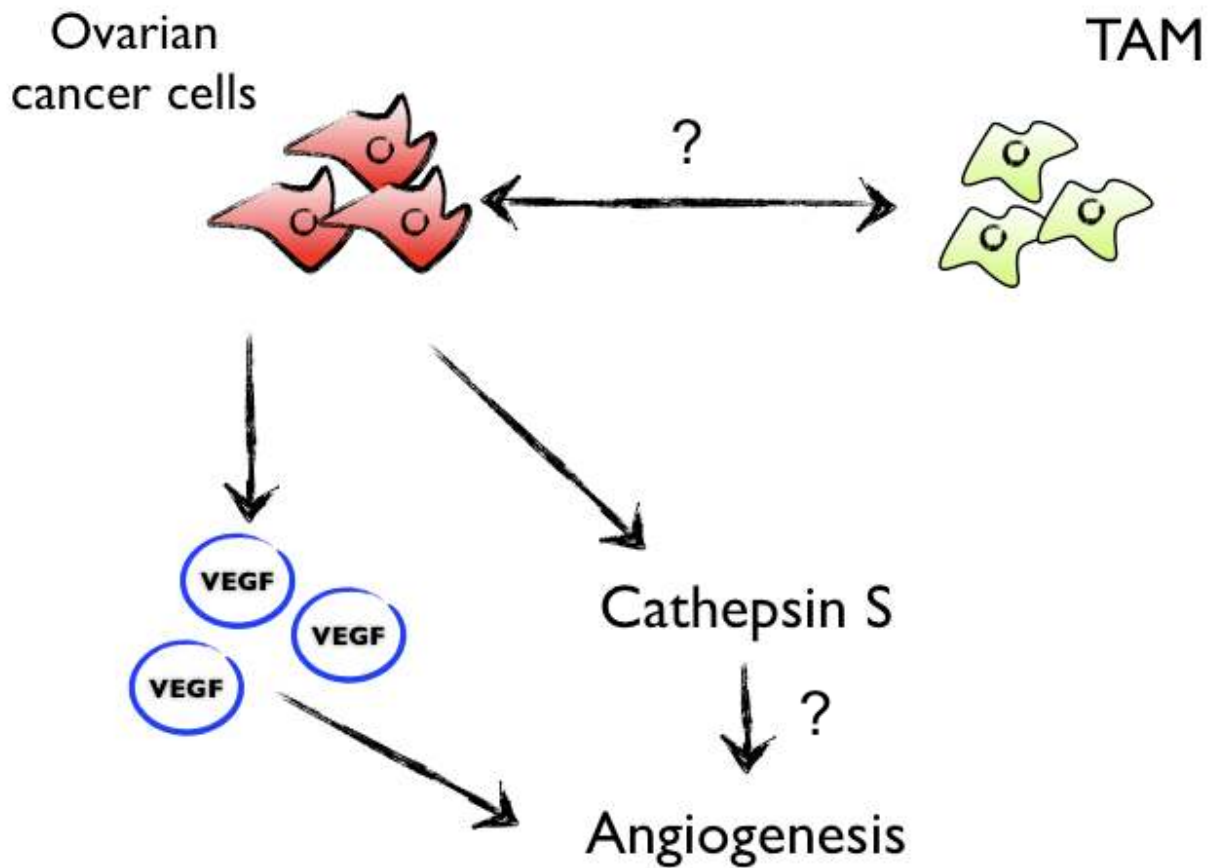


Figure 11. Proposed model for the role of tumor-associated macrophages in tumor-induced angiogenesis

In tumor microenvironment, ovarian cancer cells and tumor-associated macrophages interacted by paracrine chemokine. The interaction triggered cancer cells secreting VEGFA and the cathepsin S, and induced angiogenesis.

Supporting Information

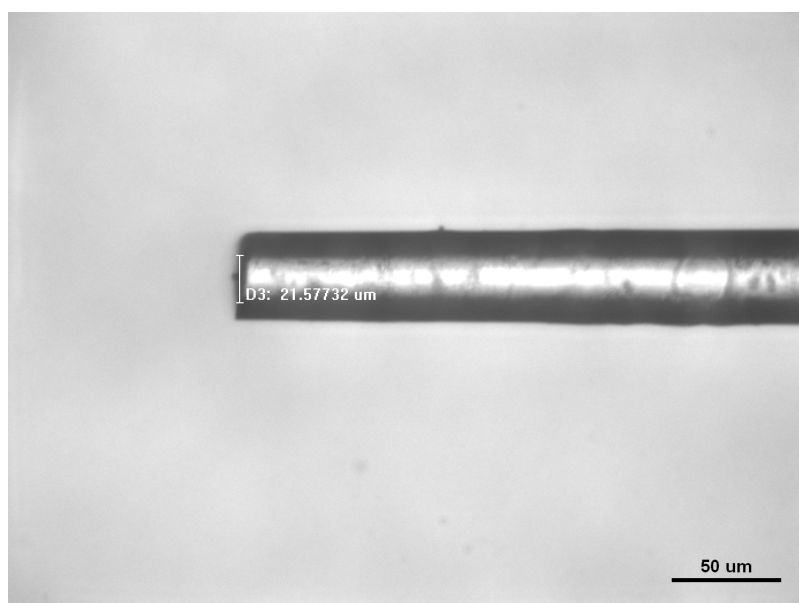
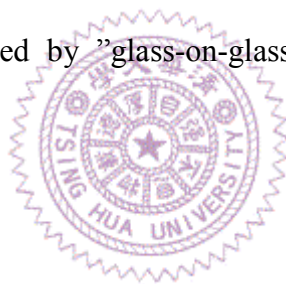


Figure S1. The tip of micropipettes was created with blunt end

The blunt end of pipette was created by "glass-on-glass" method. The open end was about 20~30μm. (Scale bar, 50 μm.)



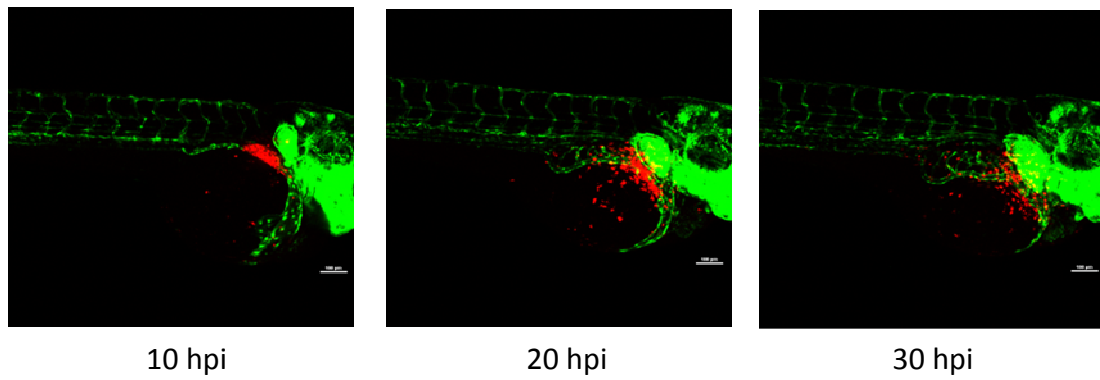


Figure S2. Time-course analysis of tumor cell dissemination throughout the perivitelline space

The ovarian cancer cells (TOV112D) were suspended in PBS and implanted into the perivitelline space near the Cuvier ducts of 2 dpf zebrafish embryos. Cell dissemination was monitored at 10, 20, 30 hours post-injection (hpi). (Scale bar, 100 μm .) Color code: Fish blood vessels are green, and DiI-labeled TOV112D cells are red.



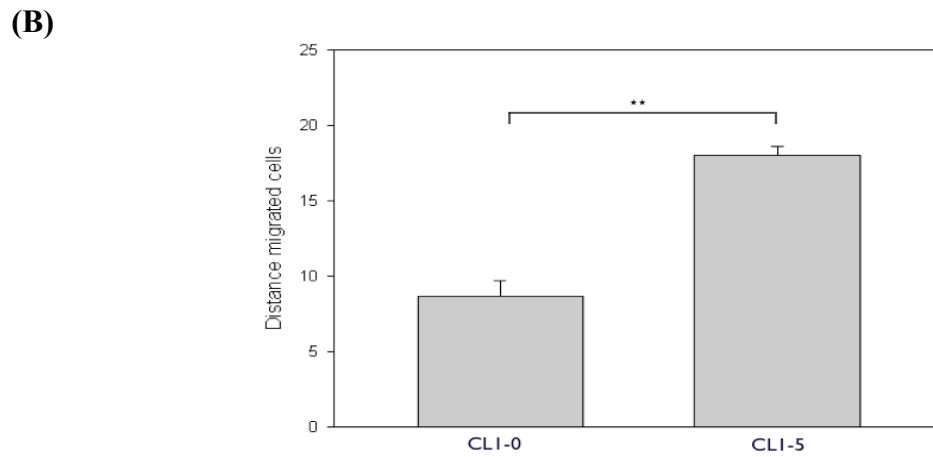
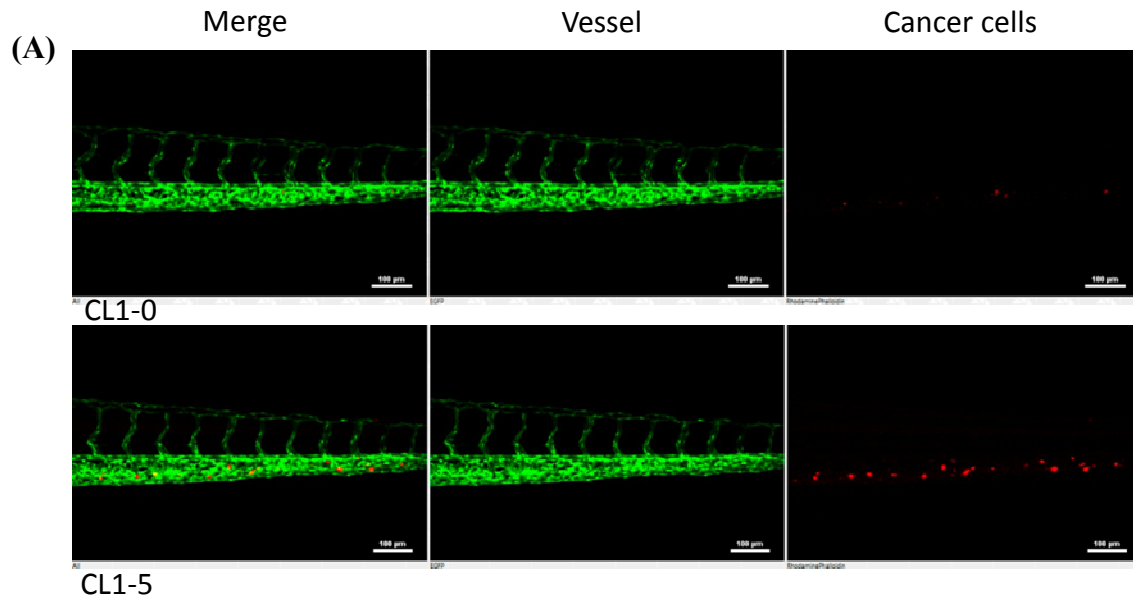


Figure S3. *In vivo* cell migration assay

CL1-0 and CL1-5 were suspended in PBS and implanted into the perivitelline space near the Cuvier ducts of 2 dpf zebrafish embryos. **(A)** Confocal image of the zebrafish tail region. (Scale bar, 100 μm .) Color code: Fish blood vessels are green, and DiI-labeled CL1-0 or CL1-5 cells are red. **(B)** Quantitative data of the migration assay. (**) $P < 0.01$ compared with CL1-0; $N=3$, and $n = 10$ embryos in each group.